ADVANCED MAGNET LAB, INC.

FINAL REPORT

SBIR - PHASE I

CONTRACT NUMBER: DE-FG02-99ER82730

BENT SOLENOIDS WITH SUPERIMPOSED DIPOLE FIELDS

-- MARCH 21, 2000 --

FINAL REPORT

SBIR - PHASE I

CONTRACT NUMBER: DE-FG02-99ER82730

BENT SOLENOIDS WITH SUPERIMPOSED DIPOLE FIELDS

TABLE OF CONTENTS

SUMMARY

During Phase I of this project a conceptual design and manufacturing technique has been developed for a superconducting bent solenoid magnet with superimposed dipole field as required in the cooling channel of a future Muon Collider. The considered bent solenoid is equivalent to a 180º-section of a toroid with a major radius of ~610 mm and a coil aperture of ~416 mm. The required field components of this magnet are 4 tesla for the solenoid field and 1 tesla for the superimposed dipole field. A magnet, operating at this field level, with the given size and shape, has to sustain large Lorentz forces resulting in a maximum magnetic pressure of about 2,000 psi.

A detailed analysis of the magnetic field in a bent solenoid with a superimposed dipole field has been performed using a special software package, CoilCAD™ that has been developed over several years at AML. This analysis has shown that it is possible to obtain the required superimposed dipole field by tilting the winding planes of the solenoid by ~ 25º.

The magnet assembly requires a large helium containment vessel for cooling with supercritical helium. This pressure vessel should meet ASME code and should be compatible with cryogenic systems at the national accelerator laboratories.

A complete structural analysis of the coil support system and the helium containment vessel under thermal, pressure and Lorentz force loads has been carried out using 3D finite element models of the structures. These studies have shown that the coil can be supported in a reinforced helium containment vessel by a series of laminated spacer blocks. The studies have furthermore shown that the coil can be sufficiently strengthened by a fiber-reinforced composite, so that the deflections in the coil, due to the Lorentz forces, are reduced to an acceptable level.

A flexible, round mini-cable with 37 strands of Cu-NbTi, developed in collaboration with the Lawrence Berkeley National Laboratory, has been selected as the superconductor. The coil has been designed to achieve an operating margin of about 25%, which should guarantee stable operation without spontaneous quenches. With the selected superconductor, six layers of cable are necessary to achieve this operating margin. Heat input to the coil from a beam tube at room temperature is intercepted by a specially designed cooling spacer, which also serves as the support structure and winding fixture for the coil.

This selected mini-cable enables the coil to be efficiently wound using the Direct Adhesive technology coupled with highly automated, computer controlled coil winding in a process that has been developed at AML. The manufacturing process has been verified by the construction of a 1/3-scale coil-winding machine for this application. This fully functional winding machine enables the manufacturing of toroidal coil sections (up to 180º) with a tilt angle of the winding planes up to 35º.

The conceptual design of the bent solenoid with its helium containment vessel is based on standard sized welding fittings to allow construction at a minimum cost. A manufacturer has been identified for the large diameter stainless steel tubes required for the inner and outer shell of this vessel. For the inner vessel, seamless 90º-sections are available, which would eliminate any concern about field distortions due to magnetized welding seams.

In summary, the main technical issues of a bent solenoid, which is considered as a dispersion generating device in a future Muon Collider, have been thoroughly studied and solutions have been worked out that can be implemented at a realistic cost. Thus we are confident that a reliable magnet of this type can be designed and built at an affordable cost. The conceptual design is readily adaptable to the construction of similar magnets with variations in size and geometry. AML is interested in applying the technology developed under this Phase I effort to magnets required for the Muon Collider R&D program and will propose to construct a demonstration magnet under a Phase II grant.

1. DESCRIPTION OF THE PROBLEM AND THE RESEARCH EFFORT

This research effort has been directed towards the development of superconducting bent solenoid magnets with a superimposed dipole field. Such magnets are required for the cooling channel for a high brightness Muon Collider[1] now under extensive study. [Such a magnet has been characterized in the Solicitation as "for dispersion generation in large emittance beams" in particle accelerators].

With the configuration in Figure 1, charged particles traversing a bent solenoid (half of a toroidal magnet) of sufficient field strength are forced into a helical path, i.e. "trapped". The trapped particles follow paths parallel to the axis of the solenoid; however, due to the magnetic gradient that is present in the toroidal field they tend to drift away from the axis. A dipole field superimposed on the toroidal field in the solenoid compensates for the drift for a given particle energy[2], and particles with different energies are dispersed.

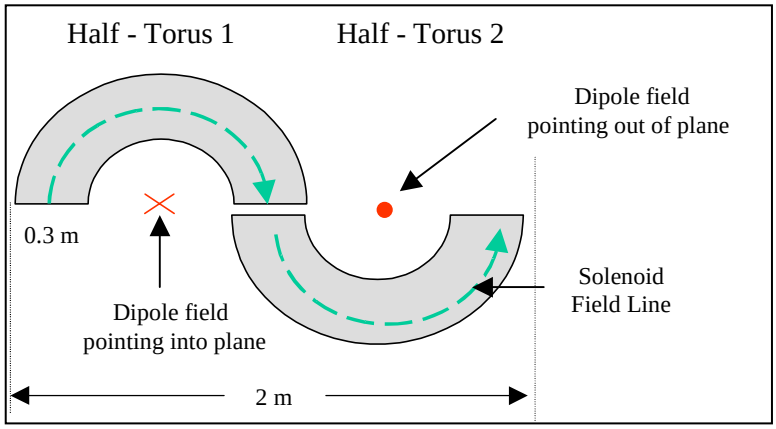

Figure 1

The required toroidal field strength is in the range of 3-5 tesla on the axis and the superimposed dipole field is in the range of 1 tesla. The aperture of the beam tube required to fit inside the magnet is about 30 cm. The aperture of the coil must be somewhat larger than the beam tube to allow for necessary components for cooling and thermal insulation of the superconducting magnet. We have selected 40 cm as the coil aperture to be used in this project.

In addition, it is expected that there will be substantial beam loss in this region of the Muon Collider[3]. Thus it will be necessary to ensure that the magnets will be sufficiently radiation hard. Energy deposition can also increase the magnet temperature and thus we assume that the operating margin should be in the 20–25% range.

The research effort during Phase I included the following:

- Liaison work to obtain specifications and requirements for the final magnet from the Muon Collider Study Group.
- Obtain properties of appropriate superconductor
- Magnetic design studies

---

[1] Muon-Muon and other High Energy Colliders, R. B. Palmer and J. C. Gallardo, Brookhaven National Laboratory, Feb. 1997.
[2] Muon Dynamics in a Toroidal Sector Magnet, J. C. Gallardo et al., Brookhaven National Laboratory – 64786-98
[3] N. Mokhov, private communication.

- Development of the conceptual design for a complete 180° bend magnet coil
- Development of the conceptual design for the coil support structure and the helium containment vessel.
- Analytical work to support the magnetic and structural design of the magnet assembly in order to meet requirements developed during the Muon Collider study.
- Design and construction of a reduced-scale winding machine model that enables the winding of the developed conductor pattern on the coil support tube.
- Develop magnet assembly concept.

2. PHASE I RESEARCH

2.1 Liaison work on requirements for the bent solenoid

The principal investigator attended a meeting about Muon Collider issues at Brookhaven National Laboratory on Sept. 10, 1999. He gave a presentation about the tilted plane solenoid coil winding concept and a description of the Phase I SBIR project. Discussions were held on suitable parameters for bent solenoid magnets that would be used in the Muon Collider cooling channel and in the targetry R&D program for a Muon storage ring.

2.2 Conductor

The conductor selected for the magnet is a 37 strand round mini cable with 1, 6, 12, 18 Cu-NbTi strands in successive layers as shown in the figure. The winding direction is successive layers is reversed, which leads to a round cross section of the cable. The cable is insulated with 0.001" thick Kapton tape wrapped around the conductor. Kapton insulation has a high radiation resistance that should be sufficient for this application.

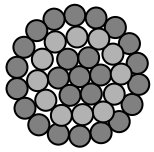

Figure 2. Schematic cable cross section

A round mini-cable is the preferred superconductor rather than a flat Rutherford-type cable for the solenoid magnet based on the following considerations:

- The round cable can be easily bent in any direction. The Rutherford-type cable requires special cable orientations to accommodate bends, as in the constant-perimeter design for coil ends of accelerator dipoles and quadrupoles.
- Preventing any voids with a flat cable in the bent solenoid geometry would be rather difficult. Unfilled voids would compromise the stability of the winding pattern and could lead to premature quenching of the coil below the critical current of the cable.
- A round cable is less expensive than a Rutherford type cable. AML has done a cost comparison between Rutherford type cable and round cable. The round cable was found to be significantly less expensive than the Rutherford type cable for equal numbers of ampere-meter.
- A round cable does not show any degradation in critical current due to the cabling process. For a Rutherford type cable a degradation of 5-10% is found.

In comparison to a monolithic conductor, a Kapton wrapped mini cable also has significant advantages:

- Helium will penetrate the Kapton surrounding the cable and will help to stabilize the conductor. Helium is more efficient in this respect than copper, due to the significantly larger specific heat of helium at cryogenic temperatures (~ 4.25 K). Thus it would take a higher energy deposition into the conductor to cause a quench in the magnet.
- The multi-strand conductor is more flexible and can be handled easily in the winding process, which reduces the manufacturing cost of the coils.
- The multi-strand cable reduces the risk of conductor failure during operation. Even if one of the strands develops a problem, the other strands can take over the current and keep the coil operational.

The described advantages have led to a recent development of a round mini cable by Lawrence Berkeley National Laboratory in collaboration with AML for applications in fusion magnets. The main goal of this cable development was flexibility of the conductor. For the bent solenoid flexibility is not of outermost importance and a cable with a smaller number of larger diameter strands could be considered. AML has based the design of the bent solenoid on this conductor. Parameters for this cable are shown in the Table.

Table of Cable Properties

Item	Value	Units
Number of Strands	37	
Strand Diameter	0.32	mm
Cable Diameter	2.25	mm
Cu/SC ratio	2.35/1	
Nominal Strand J_c @ 4.23 K, 6 tesla	2,500	A/mm^2
Filament diameter	9.8	μm
Insulation	Kapton wrap	

2.3 Tilted Coil Concept

The bent solenoid can be represented by one-half of a toroidal magnet with major radius R and minor radius a as shown in Figure 3.

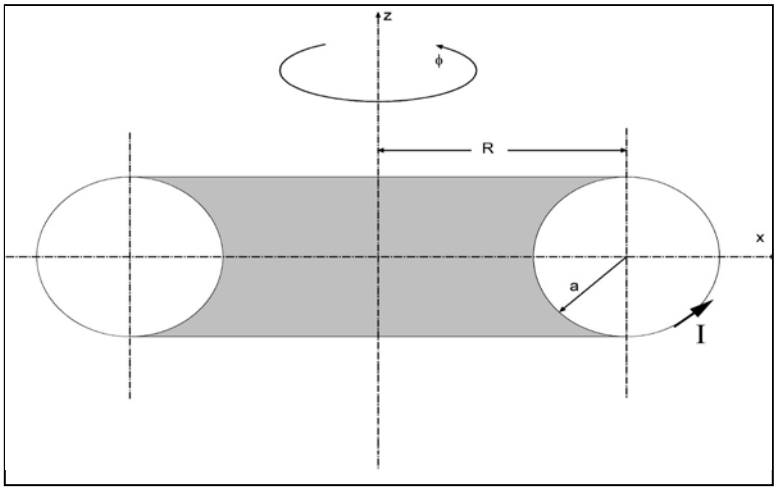

Figure 3. Bent solenoid with major radius R and minor radius a.

A surface current I produces a solenoidal field in the direction φ parallel to the axis of the torus. However, for the Muon Collider application, a superimposed dipole field is required. This could be obtained by adding a flat dipole winding to the outside of the toroidal coil as shown in Figure 4.

However, a more innovative and cost-effective approach, and the one that we propose here, is to tilt the planes of the toroidal coil in such a way that the required superimposed dipole field is obtained. The effect of tilted winding planes on the field can be illustrated with straight solenoid magnets. Figure 5 is a side view and isometric view of the generated conductor pattern for a solenoid with tilted winding planes. Field calculations reveal a pure solenoidal field for the case of the vertical winding planes and a solenoidal field with a superimposed vertical dipole field which is about 50% of the solenoid field for the 45 º tilted plane case.

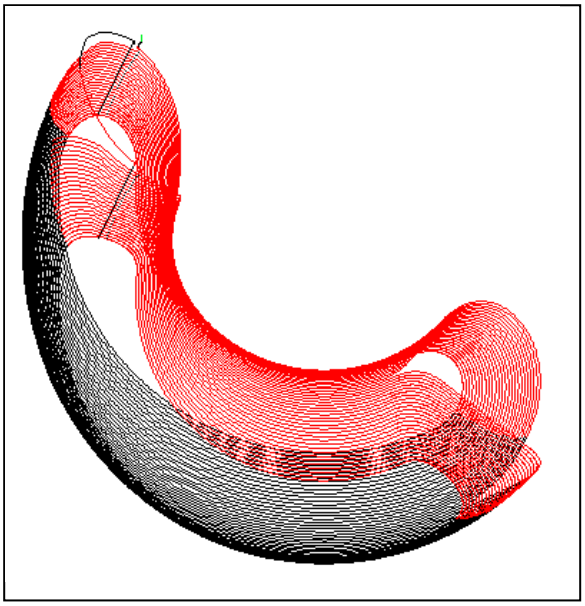

Figure 4. Flat pattern dipole winding that could be used to superimpose a dipole field on a bent solenoid.

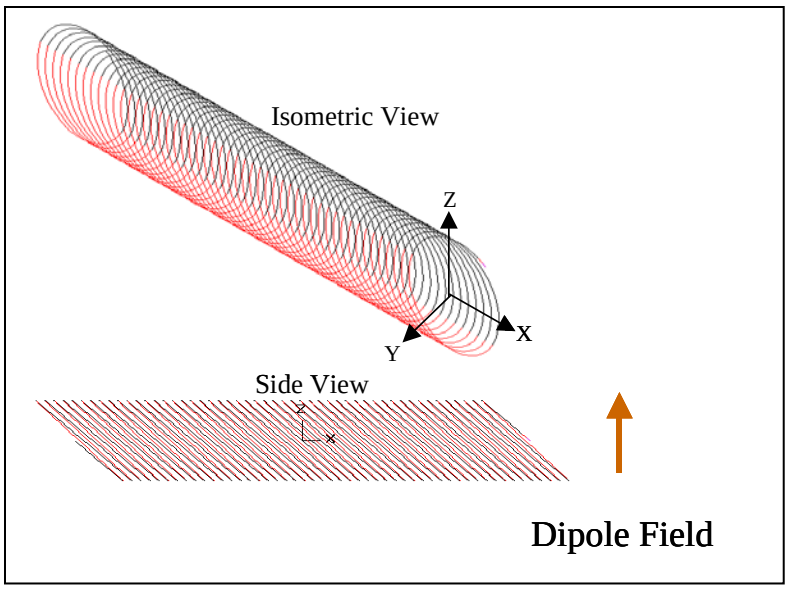

Figure 5. Straight solenoid with tilted winding planes

The tilted coil approach can be applied to the bent solenoid as shown in Figure 6. The strength of the dipole field resulting from the tilted winding planes can be adjusted by varying the tilt angle of the planes. The more the winding planes deviate from the vertical direction, the higher the relative strength of the dipole fields. For example, a tilt angle of about 25 degrees produces a ratio of 4 tesla to 1 tesla between the solenoid and the dipole fields, which is consistent with the requirements for this proposal.

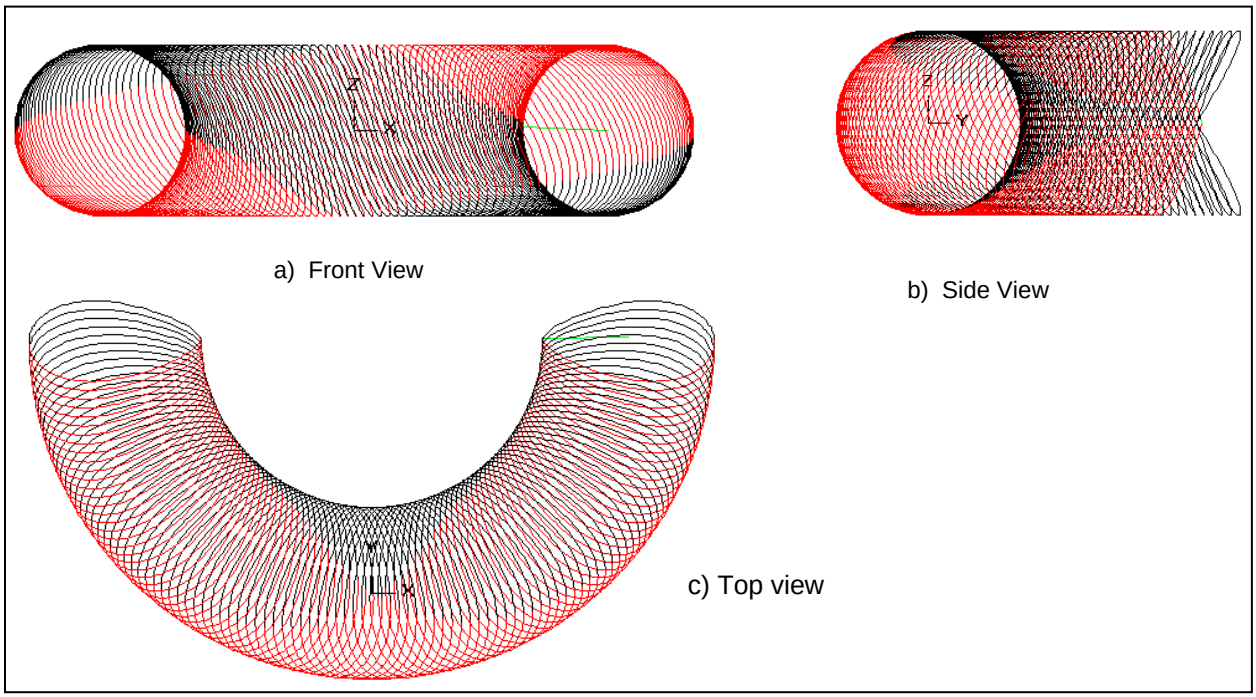

Figure 6. Bent solenoid with tilted winding planes in different views. The tilt angle of the planes is 25 degrees. For clarity the conductor pitch has been increased so that the individual turns can be seen.

2.4 Magnetic Analysis Studies

The special magnet design software, CoilCAD™, which has been under continuous development by AML for several years, has been used to develop the magnetic design of the coil. This software uses an object-oriented approach. Coil forms are selected from predefined classes, like dipole, flat pancake, solenoid, toroid, etc. A few parameters fully define the coil form of each class. After a coil has been generated, it can be transformed in many ways, (twisted, bent, stretched, etc.) to generate even the most complex coil forms. Coils generated in that way can be combined to larger objects. Without any user programming CoilCAD™ generates the complete 3-D space curve of the conductor and from this space curve calculates the 3-D field at any point. Thus, CoilCAD™ can be used to compute the fields in a bent solenoid with tilted coils or in non-tilted solenoid coils with a dipole winding.

The fields of accelerator steering and focussing magnets are normally treated as two dimensional and described as multipole decompositions, i.e., the magnetic field is given as the superposition of dipole, quadrupole, sextupole, etc. fields. Details of this analysis can be found in many articles and textbooks[4].

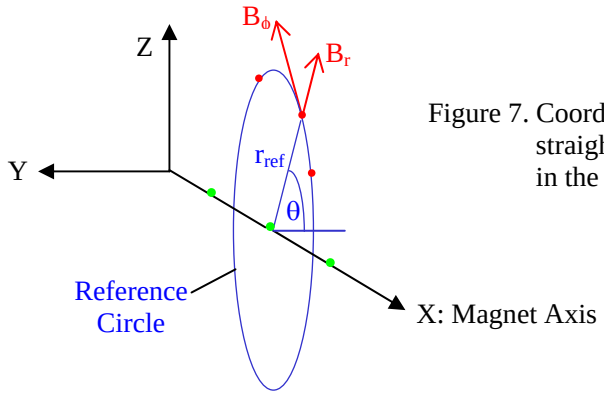

Figure 7. Coordinates used to calculate the multipole content of straight (2-D) accelerator magnets. The magnet axis is in the X direction.

As indicated in Figure 7 the field components B_r and B_ϕ in the plane of the reference circle are calculated for a number of points on a certain reference radius r_{ref}. A Fourier analysis of these fields yields the multipole components for the chosen reference radius. These multipole fields are in respect to the center of the chosen reference radius, i.e., all multipole fields except the dipole are zero on the chosen center. If this multipole analysis is performed for different points along the axis of the magnet (see Figure 7), also the fields in the ends of a magnet can be conveniently described.

CoilCAD™ uses the Biot-Savart law to calculate the fields on a chosen reference circle and performs the Fourier analysis to calculate the multipole content. CoilCAD™ can perform this analysis automatically for a chosen range of x values along the axis of the magnet. A comparison between CoilCAD™ results and analytic calculations typically shows agreement in more than 6 digits, indicating the high precision of these results.

We have generalized the conventional multipole analysis to describe bent magnets with the same formalism. The axis of the magnet is no longer a straight line, but a circle. Accordingly, the fields are calculated on a reference circle in the plane perpendicular to axis of the bent magnet (see Figure 8). A Fourier analysis of the two orthogonal field components B_r and B_ϕ in this plane yields multipole components, which describe the field at that bend angle. Calculating these multipole components for different bend angles gives a complete description of the bent solenoid field. As for straight (2-D) coils, the resulting multipoles are in respect to the center of the used reference circle.

[4] R. Meinke, P. Schmueser, Y. Zhao, Methods of Harmonics Measurements in the Superconducting HERA Magnets and Analysis of Systematic Errors, DESY-HERA-91-13.
Superconducting Accelerator Magnets, K.-H. Mess, P. Schmueser, S. Wolff, World Scientific 1996,

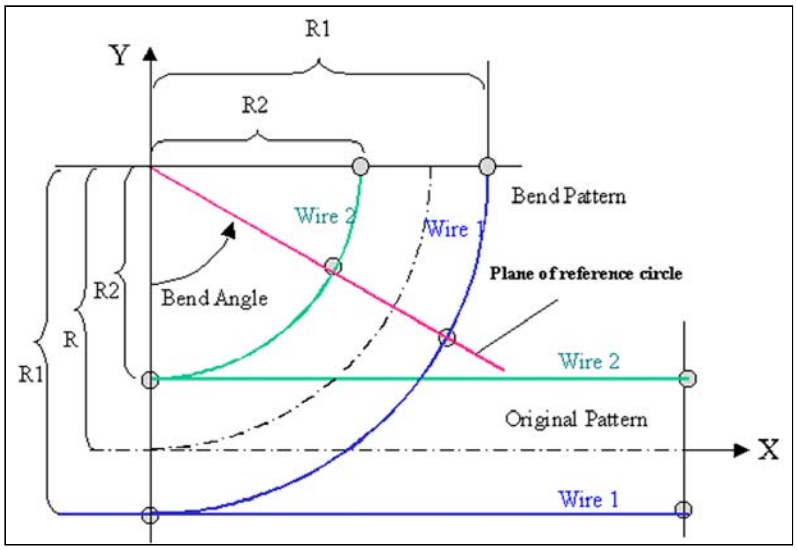

Figure 8. Diagram of geometry used by CoilCAD™ for bent magnets. The original straight patter is bent in the X – Y plane as shown in the diagram. The red line indicates the intersection of the plane of the reference circle with the x-y plane. The field components B_r and B_ϕ in this plane are used for the Fourier analysis to calculate multipole fields.

As for the straight coils, CoilCAD™ automatically calculates the multipole content of a given coil for a set of bend angles. For a large aperture magnet like the bent solenoid the field extends significantly to the outside of the coil at both ends. CoilCAD™ therefore extends the coil axis with a straight line at both ends and performs the field calculations along these extensions as shown in the following sketch (Figure 9). In the diagrams shown later the fields are normally plotted as a function of arc length. This "arc length" is defined as shown in figure 9 and extends to the outside of the coil at both ends and has zero in the middle of the arc.

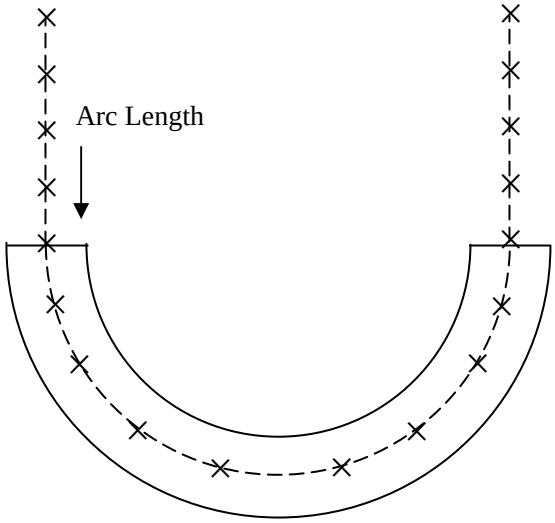

Figure 9. The axis of the bend is indicated by a dashed line. Arc length is measured along this line, which extends in a straight line at both ends.

It is important to point out that the generalized multipole analysis, developed here for the bent solenoids, enables a direct comparison between the magnetic fields of straight and bent coils. It also allows calculating directly the superimposed dipole field for the bent solenoid.

The magnetic analysis of the bent solenoid was performed in several stages on progressively more complex coils in order to understand the field variations between them, particularly from the effect of using tilted winding planes for the coils. To reduce computing time, this study used a simulated coil configuration consisting of a single layer coil with 500 turns. It was verified that the number of layers and turns has no significant effect on the calculated fields. In all cases the current was adjusted to give nominal fields of 4 tesla.

The presented field calculations are done for two different reference radii: $r_{ref} = 0$, the solenoid axis, and $r_{ref} =$ 140 mm, which is about 2/3 of the coils aperture; the position for which field quality of accelerator dipoles and quadrupoles is most often evaluated.

The configurations studied were the following:

- A straight solenoid with non-tilted winding planes.
- A straight solenoid with tilted planes to obtain the superimposed dipole field.
- A bent solenoid of 180º with non-tilted winding planes.
- A bent solenoid of 180º with planes tilted at 25º to produce the superimposed dipole field.
- For comparison, a bent solenoid of 180º with non-tilted coils with a one-layer dipole pattern winding on its surface to produce the superimposed field.

The results are discussed in the following topic headings.

Effect of tilted winding planes in a straight solenoid:

The parameters used to study this case are shown in the following Table.

	Straight solenoid	Tilted coil solenoid
Coil ID [mm]	416.4	416.4
Number of conductor layers	1	1
Number of turns	500	500
Conductor diameter [mm]	2.35	2.35
Coil current [A]	12,200	12,200
Nominal field [tesla]	4	4
Winding pitch [mm]	3.83	3.83
Resulting coil length [mm]	1915	1915 (center line)
Tilt of winding plane [deg]	0	25

The chosen winding pitch defines the length of the solenoid. The resulting value of 1,915 mm is equivalent to the arc length of the bent solenoid analyzed later.

The following Figures show some of the results obtained for the straight magnets. Of interest for both the tilted and non-tilted coils is the drop off in field near the ends and the higher order multipole field at the coil ends.

Figure 10 shows the field component B_X (parallel to magnet axis) at $r_{ref} = 140$ mm. For the straight coil B_X can be taken as the solenoid field. Its value is 3.915 tesla. This is the same as the field calculated on axis ($r_{ref} = 0$ mm) as expected for a solenoid magnet. The solenoid field B_X for tilted winding planes (with graph points shown as circles) and non-tilted winding planes (with graph points shown as squares) are almost identical at the reference radius of 140 mm. Note that the field drops off rapidly at the end. This drop starts at x ~ 600 mm, which is about two-thirds of the way to the end of the magnet.

The dipole field at $r_{ref} = 140$ mm along the length of the magnet for the coil with tilted planes is shown in Figure 11. The dipole field in the center of the coil (x = 0 mm) is 0.951 tesla.

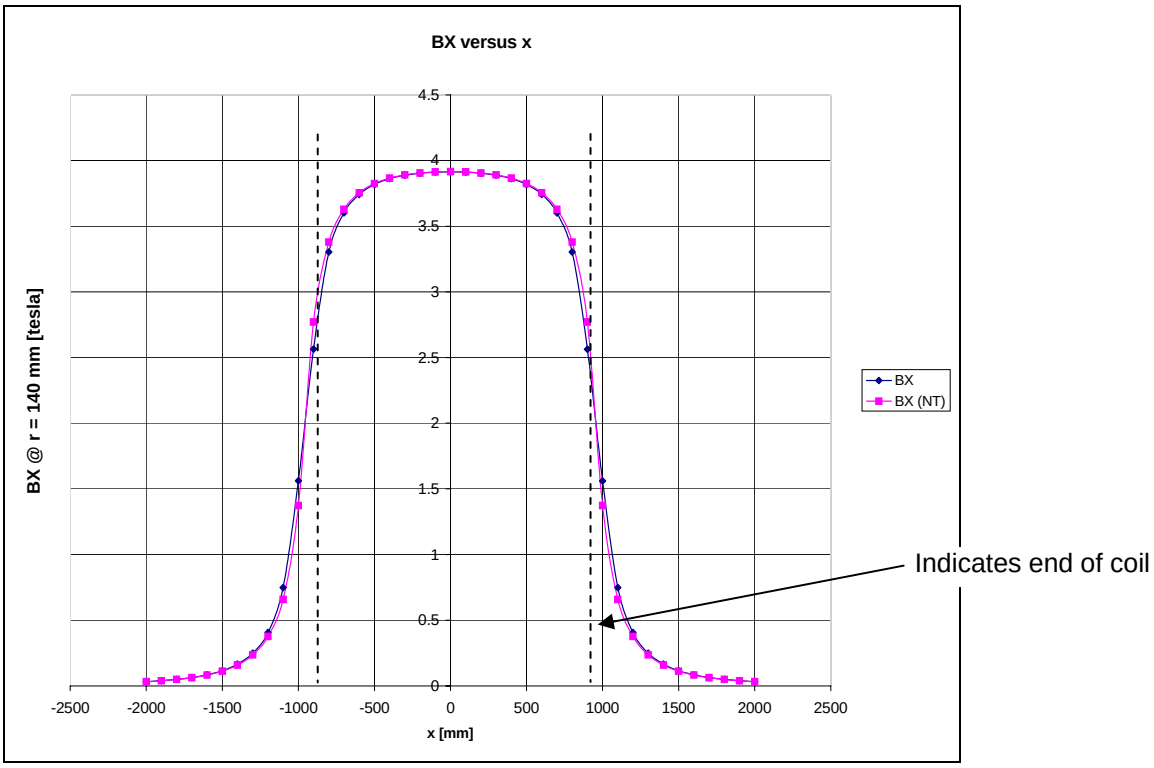

Figure 10. Solenoid field (B_x) in tesla along the length of a straight solenoid coil for tilted (black) and non-tilted winding planes (purple).

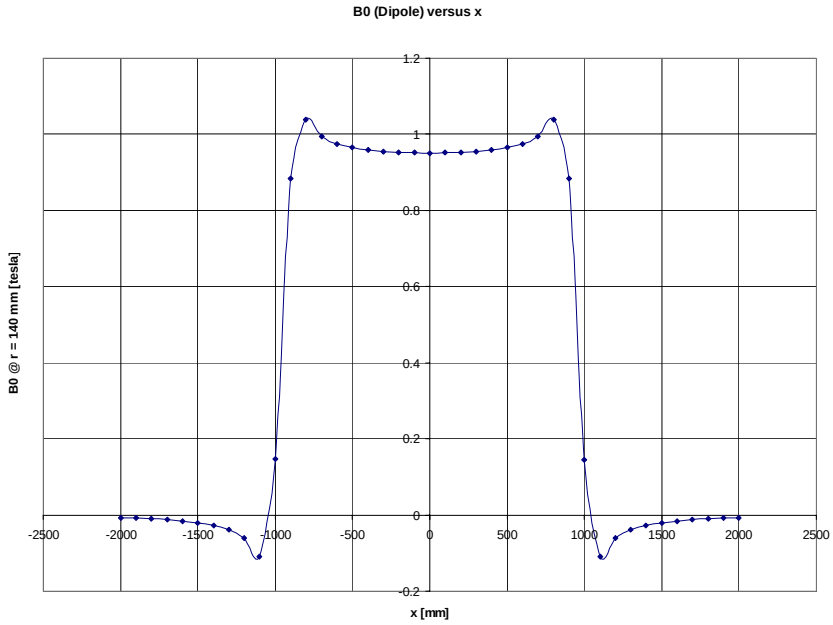

Figure 11. Dipole field (B0) in tesla along the length of a straight solenoid with tilted planes at a reference radius of 140 mm.

The quadrupole fields (normal and skew) along the length are shown in Figure 12 for the solenoid with tilted planes. A significant skew quadrupole component is found at the coil ends, which is caused by the asymmetry due to the tilted planes. As expected the sign of the skew quadrupole is different at the two ends, because the conductors extend further on the top at one end and further on the bottom at the other end.

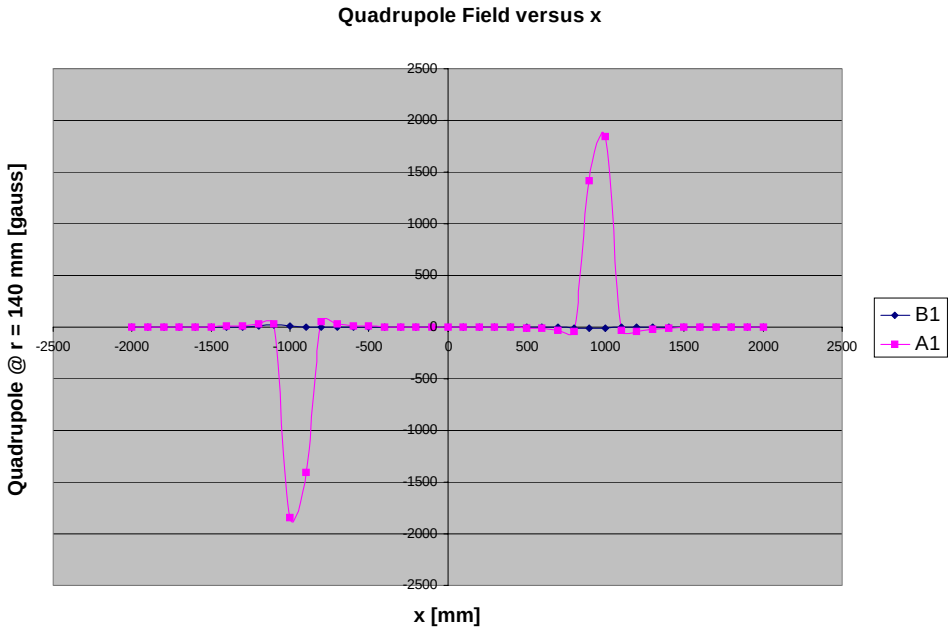

Figure 12. Normal (B1) and skew (A1) quadrupole fields in gauss along length of straight solenoid with tilted planes.

CoilCAD^{TM} automatically calculates all multipole fields up to a requested order. For the straight solenoids all multipole fields are completely negligible in the body of the magnet. The lower-order multipole fields show significant contributions in the coil ends. For example the normal and skew sextupoles (r_{ref} = 140 mm) are shown in Figure 13. The observed sextupole component changes sign within each coil end and the sextupole field integrated over each end individually cancels almost completely.

.

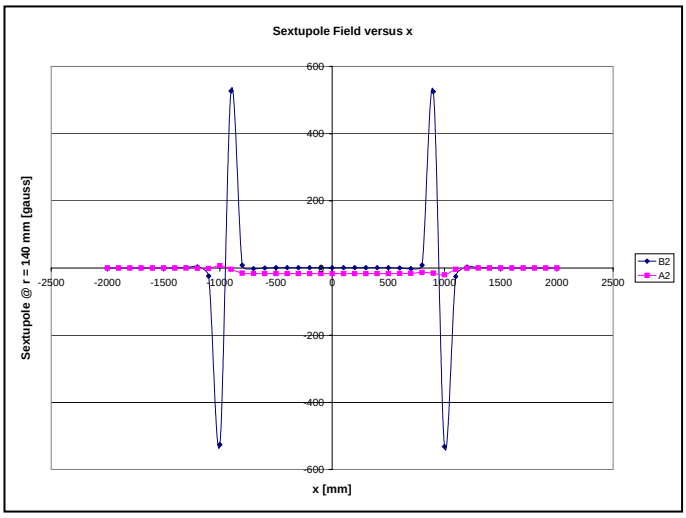

Figure 13. Normal (B2) and skew (A2) sextupole fields in gauss along the length of a straight solenoid with tilted planes.

Bent Solenoid Field Calculations

Before presenting the results of the bent solenoid field calculations it is helpful to review the theoretical description of the field in a toroidal magnet since the bent solenoid can be considered as a segment of such a magnet.

Consider an ideal circular-cross-section torus, as shown in Figure 14 that is energized with a surface current sheet. The surface current occupies zero thickness and flows around the torus perpendicular to the toroidal direction, φ.

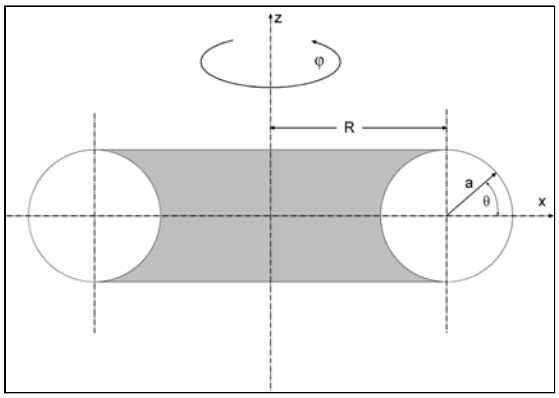

Figure 14. Diagram of toroidal magnet. Equatorial plane is the X-Y plane.

The current sheet can be approximated by N closed current loops, perpendicular to the toroidal direction. For example, the following parameters produce a central solenoidal field of 4 tesla in a torus with dimensions considered for the bent solenoid. However, the actual magnet will have a multi-layer coil so that the transport current can be reduced to a more economical level.

Number of turns, N	2440
Current, I	5000 A
Minor axis, a	203.3 mm
Major axis, R	609.6 mm

The field along the center axis of a toroid of major radius R with a uniform current distribution has only an azimuthal component, B_φ, given by:

$$B_\varphi = \frac{\mu_0 NI}{2\pi R} = 4.003 \text{ T}$$ (using values from the above table)

For a horizontally oriented torus (perpendicular to the z-axis), the field at any point inside the torus is independent of the vertical position (z-coordinate). The field strength in any vertical band can be expressed in terms of the toroid's major radius R, its minor radius a, and the angle θ (see Figure 14), which is the angle to the surface point at the top of the band. (Thus x = a cos θ is the horizontal distance from the central axis.) Since the total enclosed current is the same for any circle of radius from R-a to R+a, we can substitute r(θ) = R + a cos θ into the above equation and get the relationship for the field strength at points other than the central axis:

$$B_\varphi(\theta) = B_\varphi \frac{R}{R + a\cos\theta}$$

Thus, the field is stronger at the inner radius of the torus (θ = 180 degrees) than at the outer radius (θ = 0 degrees). Also, when R is very large compared to a, the configuration resembles sections of straight solenoids and the field approaches B_φ everywhere. The variation of B_φ with distance from the center axis is shown in Figure 15 for a toroid with the parameters given in the table above. It is seen that when the ratio of (R+a) / (R-a) is 2:1 as in this example, the field is twice as strong at the inner radius of the torus as at the outer radius.

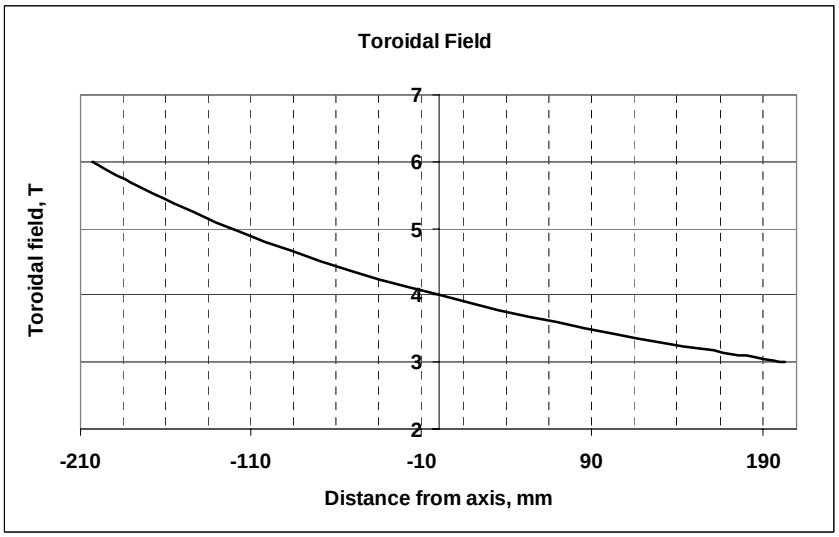

Figure 15. Field variation horizontally across toroidal magnet.

Detailed field calculations have been performed with CoilCAD™. The coil is simulated by first generating a straight coil of appropriate length and then introducing a 180° bend (see also Figure 8). The coil parameters used for the calculation are listed in the following Table.

Coil ID [mm]	416.4
Bend radius [mm]	609.6
Total bending angle [deg]	180.
Number of conductor layers	1
Number of turns	500
Conductor diameter [mm]	2.35
Min. winding pitch [mm]	3.83 Is this along the centerline?
Resulting coil length [mm]	1,915
Tilt of winding plane [deg]	25 and zero for comparison
Coil current [A]	12,200

The total field along the axis is shown for the case of 25º tilted coils in Figure 16 where it is plotted at several radial distances from the axis. Note that the field values along the inner radius and the outer radius are quite similar to those obtained from the previous formula for the field in a toroidal magnet. Figure 17 is the plot of the field across the equatorial plane and is quite similar to that in Figure 15 for the classical toroidal magnet. A comparison with a bent solenoid with non-tilted planes has shown that the absolute fields and the gradients are almost identical for both cases.

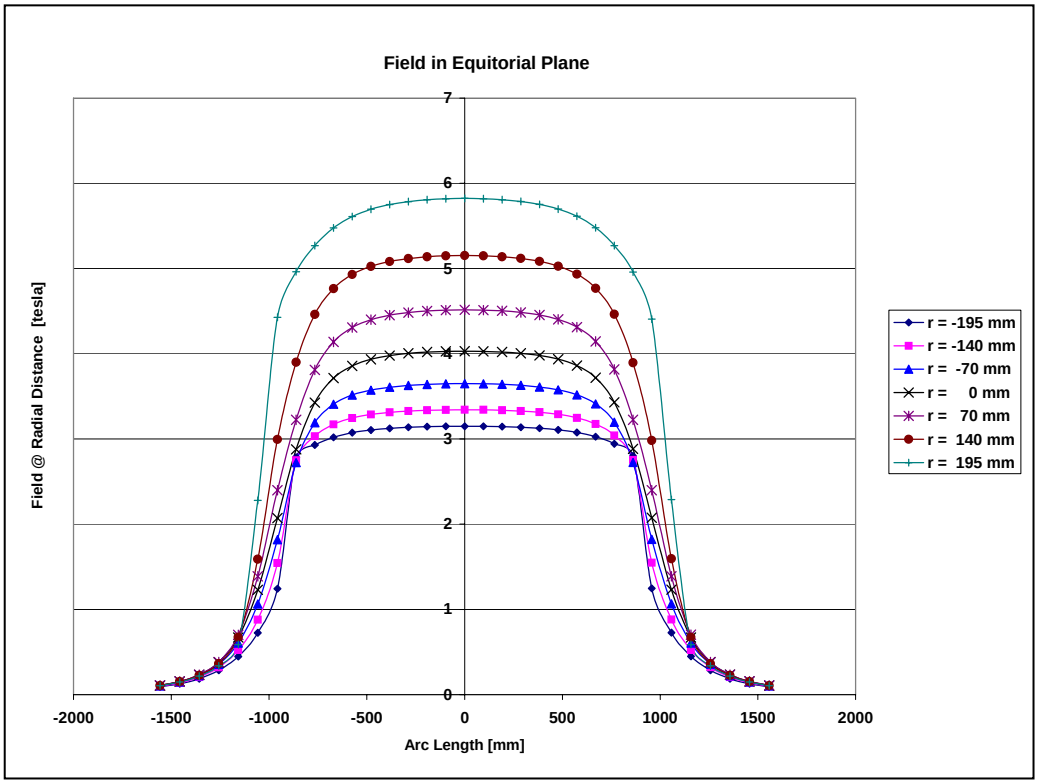

Figure 16. Field along the axis in equatorial plane of bent solenoid with tilted planes at different radii.

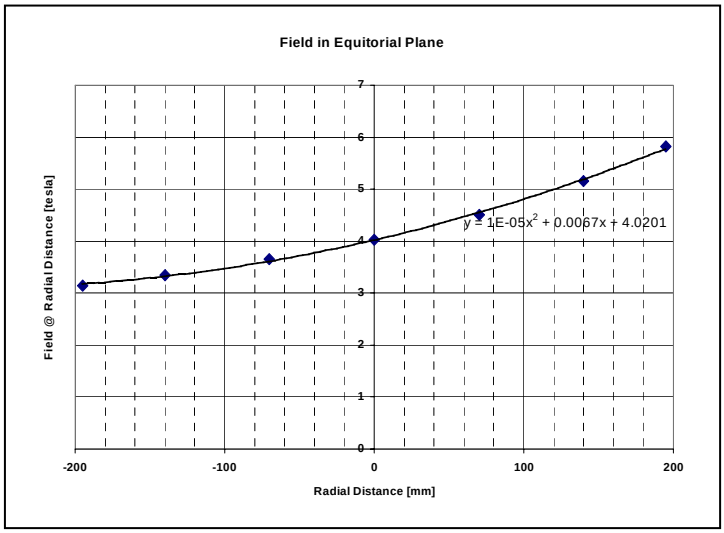

Figure 17. Field variation in equatorial plane for bent solenoid with tilted coils. Negative direction is toward the outer radius of the solenoid. The solid curve is a fit of a quadratic function to the data.

The bent solenoid with a tilted coil shows a superimposed dipole field of about 0.93 tesla in the center (see Figure 18). The dipole field increases to about 1.01 tesla very close to the end of the coil. The dipole field shows a very rapid decrease to zero over a distance of about 150 mm.

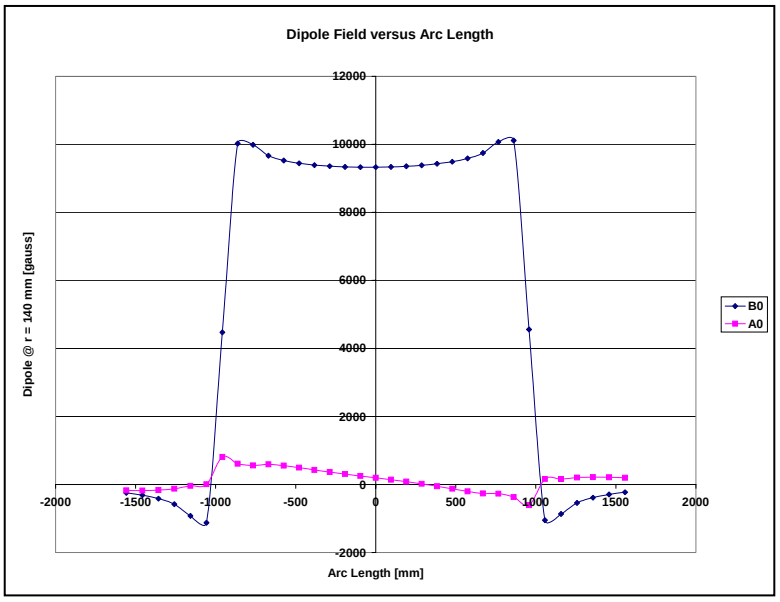

Figure 18. Normal (B0) and skew (A0) dipole fields along the length of the bent solenoid with tilted coils.

As already observed for the straight solenoid, higher-order multipole components are present at the end of the solenoid. The strongest multipole field in the case of tilted planes is the skew quadrupole, which peaks at about 0.2 tesla (see Fig. 19). In comparison, the skew quadrupole for the non-tilted planes (not shown) peaks at only about 0.03 tesla. This larger skew quadrupole for the tilted planes is caused by the asymmetry of the coil ends, which are tapered due to the tilt of the winding planes.

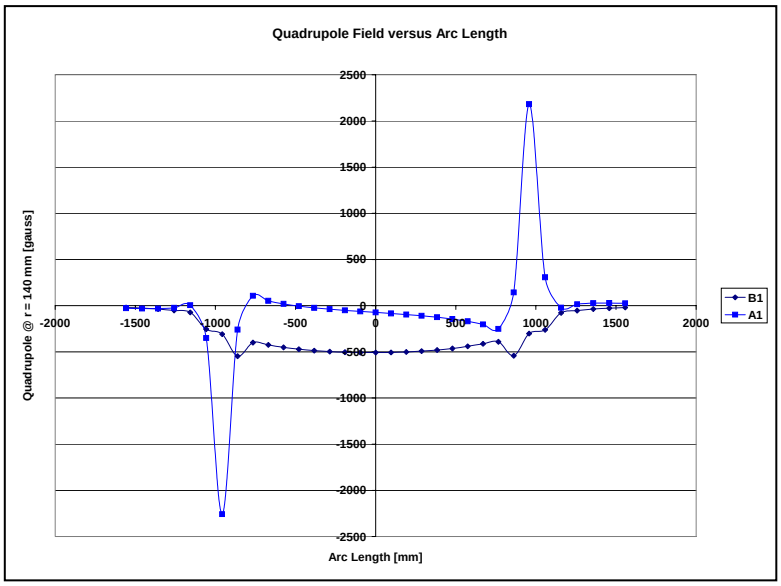

Figure 19. Normal (B1) and skew (A1) quadrupole field along the length of the bent solenoid with tilted coils.

It should be pointed out that the quadrupole calculated in this multipole analysis is not responsible for the observed field gradient between the inner and outer radius (see Figure 16). The center of the calculated quadrupole field component is on the axis of the solenoid (see description of multipole analysis on page 10), while the gradient in the bent solenoid field is monotonic between the boundaries of the coil.

The multipole fields of higher order than the quadrupole are significantly smaller and reach peak fields of less than 1% of the dipole field.

(A complete set of all multipole plots for all coil configurations exists and can be provided on request.)

Bent Solenoid with non-tilted coils using a separate dipole winding

A straight dipole magnet has been modeled with CoilCAD and then transformed into a 180-degree bend (see Figure 20).

The length of the dipole was chosen to be equal to the arc length of the axis of the bent solenoid.

The transport current was chosen to generate a dipole field of about 1 tesla. For these field studies, it is irrelevant whether the coil could be operated at this field with the given conductor. However, at a field of about 1 tesla, the critical current of the selected conductor is more than 7000 A.

The multipole content was calculated along the arc length of the magnet, in the same way as for the bent solenoid. The conductor spacing was optimized to adjust the sextupole field (the first allowed multipole component) to zero. No attempt has been made to bring the second allowed multipole (the decapole) to zero. Also, no optimization of the field quality in the coil ends has been done.

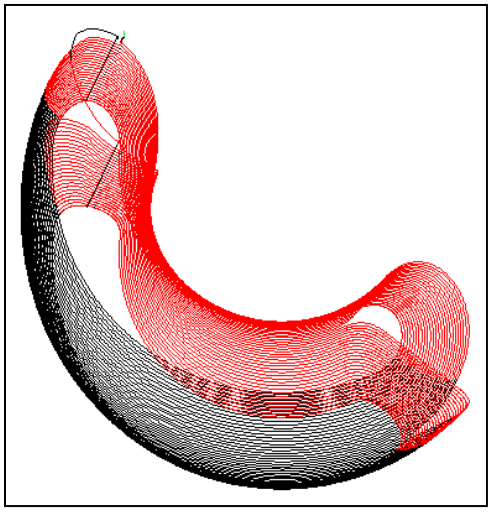

Figure 20. Coil pattern for a bent dipole winding placed over the solenoid to produce the superimposed dipole field in a bent solenoid with non-tilted coils. The conductor spacing in the figure is increased to improve the clarity.

The dipole field produced by the separate winding has been compared to that produced by the tilted coil winding. This comparison is shown in Figure 21.

The dipole field strength has been adjusted to the dipole field of the bent solenoid with tilted winding planes, i.e., about 0.93 tesla in the center of the bend. The plot of dipole field versus arc length shows a similar shape to that of the bent solenoid. The dipole field for the bent solenoid is slightly wider, but this could be adjusted by lengthening the bent dipole coil. The small skew dipole component observed in the bent solenoid is absent in the dipole, as expected for a dipole geometry with correct symmetry.

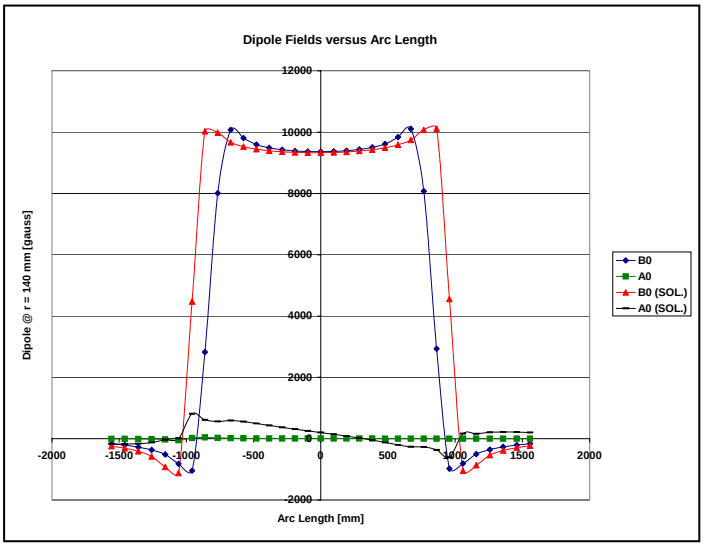

Figure 21. Normal (B0) and skew (A0) dipole field components along the length of a bent dipole. The field is calculated at a reference radius of 140 mm. The current has been adjusted to reproduce the dipole field of the bent solenoid with tilted winding planes. For comparison, the field of the bent solenoid is also plotted, indicated by (SOL).

Multipole fields along the magnet axis have been calculated for the bent dipole coil and can be compared with the fields of the bent solenoid with tilted planes. As an example the sextupole fields of the bent dipole are compared with the bent solenoid in Figure 22.

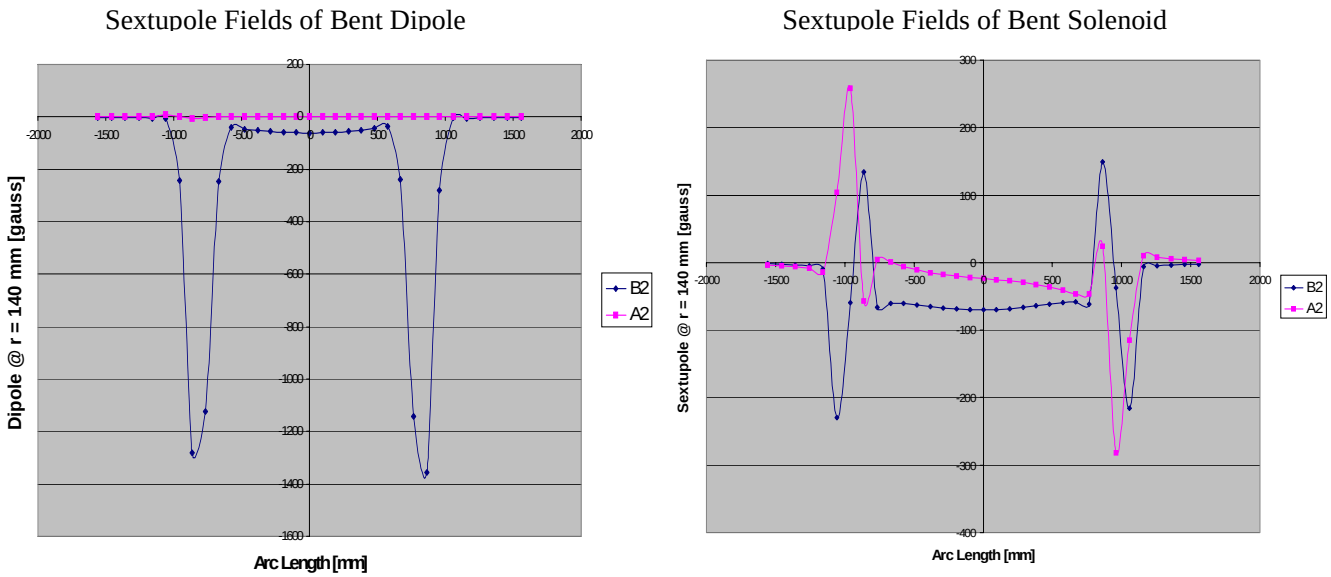

Figure 22. Normal and skew sextupole fields at r_{ref} = 140 mm in gauss of the bent dipole (left) and bent solenoid (right) along the axes of the magnets.

The normal sextupole of the bent dipole peaks at about 1300 gauss, while the bent solenoid normal sextupole in the coil ends peaks at only 250 gauss. It would be possible to improve the coil ends of the bent dipole with spacers and reduce the large observed sextupole fields to the values found for the bent solenoid, but at extra expense.

The only significant difference between the field harmonics of the bent dipole and the bent solenoid with tilted winding planes is the skew quadrupole component, which is present in the solenoid (see Figure 19). If the skew quadrupole of the bent solenoid with tilted planes were acceptable, this would be the preferred solution, since it is significantly simpler to build than the bent solenoid with the extra bent dipole coil.

Fringe field calculation

Iron shielding has not been applied to the conceptual design presented for the bent solenoid. However, the spacer blocks that support and position the coil are to be made from iron laminations and would contribute to some field enhancement and reduction of the fringe field. Thus, this type of calculation will be performed in the detailed magnetic field analysis in Phase II.

The following results were obtained for the fringe field of the magnet without shielding present. Figure 23 shows the fringe field for the bent solenoid with tilted winding planes at radial distances of 305 and 500 mm. For comparison, Figure 24 shows the result of superimposing the fields for a solenoid with straight planes and an independent dipole winding on top. The field at 500 mm exceeds 7000 gauss over a large range of the bend; this is more than twice the fringe field of the bent solenoid with tilted planes.

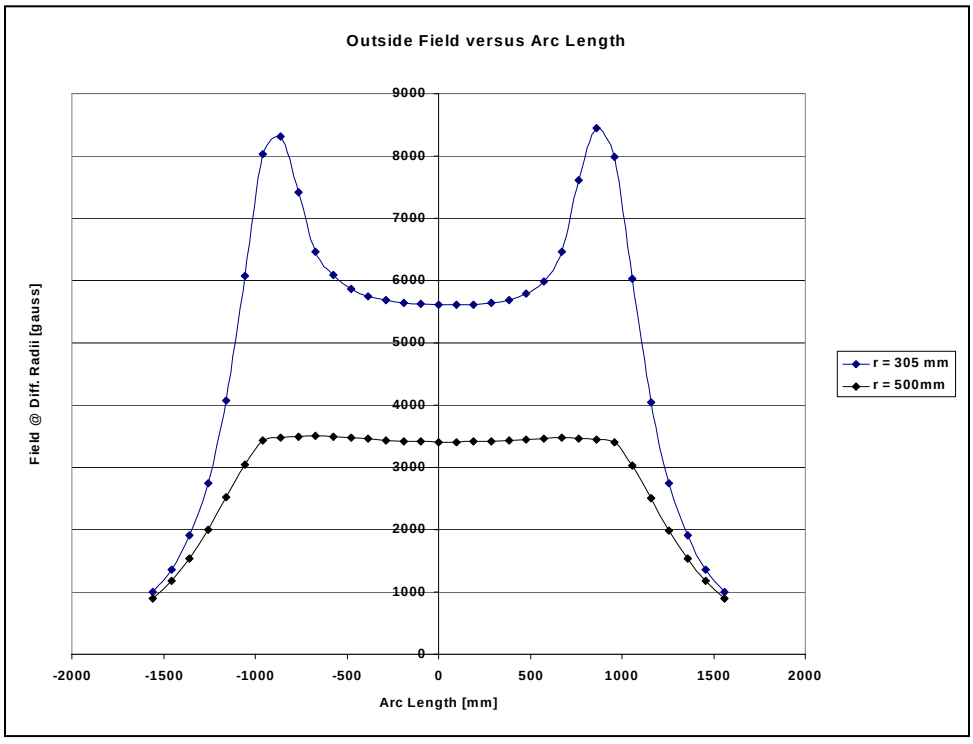

Figure 23. Fringe field in gauss along the length of a bent solenoid with tilted winding planes for radial distances of 305 mm (close to helium containment vessel) and 500 mm.

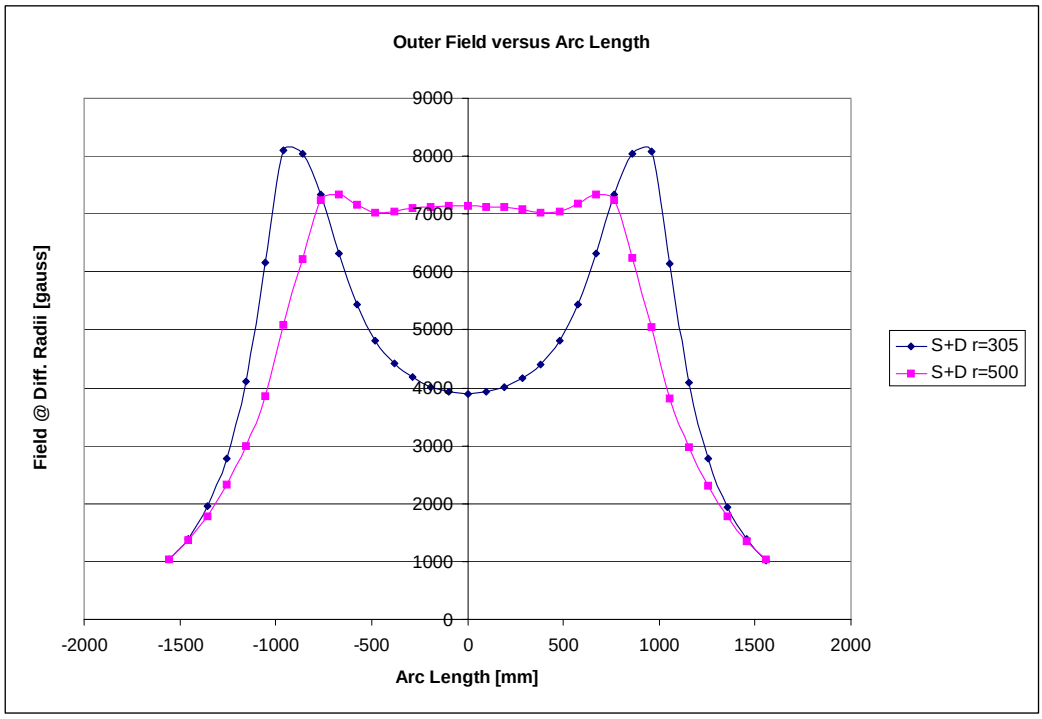

Figure 24. Fringe field along the length of a bent solenoid with non-tilted winding planes and a separate dipole layer for radial distances of 305 mm (close to helium containment vessel) and 500 mm.

2.5 Design of the Coil

The magnetic field calculations in the previous sections give a precise description of the magnetic field in the straight and bent solenoids with tilted and non-tilted coils. The results of these calculations indicate that the tilted-coil may be the best approach to obtain a 4-tesla solenoid field with a superimposed 1-tesla dipole field.

The actual coil design will use the 37-strand cable described in Section 2.2. In order to obtain an operating margin of ~ 25%, the operating current should be 1440 A. Thus six layers are required in order to produce a nominal solenoidal field of 4 tesla. The layers will be wound with a 25º tilt to produce the desired 1-tesla dipole field.

A composite tube (cooling tube) made from fiber-reinforced radiation resistant epoxy forms the base upon which the bent solenoid coil is wound. The superconducting cable will be wound onto this support tube using AML's Direct Adhesive technology, which has been developed under a previous SBIR (DOE Grant No. DE-FG02-97ER82312). This technology enables precise, computer-controlled conductor placement on a support structure. The adhesive system used in this process gives instantaneous bonding during conductor placement and structural bonding in a final curing process of the completed coil.

The cable properties and operating conditions are summarized in the table.

Operating current, A	1440
Number of strands in cable	37
Strand diameter, mm	0.32
Cu/NbTi	2.26
Cu area in cable, mm^2	2.06
NbTi area in cable, mm^2	0.913

J in Cu @ operating current, A/mm^2	698
J in NbTi @ operating current, A/mm^2	1578
Max conductor temperature, K	4.6
Estimated Max field on conductor, T	6.0
J_c degradation in cable	0
J_c of strand @ 4.23K and 6 T, A/mm^2	2500
J_c at max temperature and field, A/mm^2	2107
Operating margin	25%

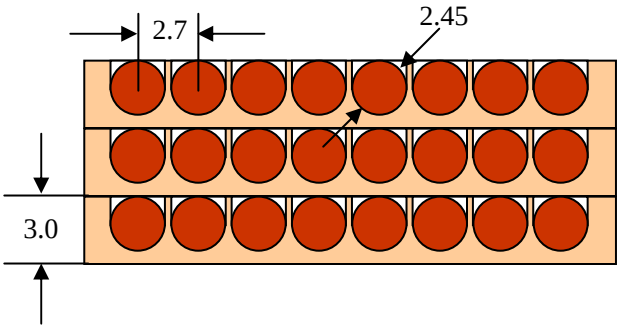

Figure 25. Schematic cross section through coil (only 3 out of 6 layers shown). The composite overwrap of each layer is machined to provide U-grooves for the next layer. Dimensions are mm.

Figure 25 shows a cross section of the coil with a winding pitch of 2.7 mm along the axis. For a straight solenoid with a single current sheet with a diameter of 416.4 mm the magnetizing force is 3.2×10^6 A/m. (370.37 turns/m/layer × 6 layers ×1440 = 3.2×10^6 A/m). This magnetizing force produces a nominal field of 4 T in this straight solenoid.

We know from theory that if the solenoid is bent into the form of a toroidal magnet with a single current sheet with a magnetizing force of 3.2×10^6 A/m, the axial field will be the same as that in the straight solenoid; i.e. 4 T. If the inner radius is ½ the outer radius, as in our configuration, the peak field at the inner radius of the torus will be 6 T. Thus, we can use the theoretical value of peak field for a conservative approach to the margin calculation. A detailed magnetic field calculation will accompany the optimized coil design for the particular magnet configuration chosen for the Phase II effort.

As indicated above, 6 conductor layers are used to obtain a nominal field of 4 tesla in the solenoid field. The conductor in each layer is placed in precisely machined U-grooves. The first conductor layer is placed in grooves that are machined into the composite coil support tube. Each layer is overwrapped with epoxy impregnated fiberglass, which is then machined to have the grooves for the next layer. A cross section is indicated in Figure 25. This technique is ideally suited to prevent conductor motion under the influence of Lorentz forces.

A specially designed winding machine has been developed for this operation and is described in Section 2.7.

After the 6 conductor layers have been wound on the coil, a layer of fiberglass reinforced epoxy, approximately 8 mm thick, will be applied to the coil to provide structural reinforcement to resist the Lorentz force load. (The structural requirements are discussed in Section 2.5.)

2.6 Magnet Support Structure and Helium Containment

The magnet assembly consists of the coil assembly, its support structure, and the helium containment vessel necessary to achieve the cryogenic environment for the superconductor. The proposed configuration is shown in Figure 26.

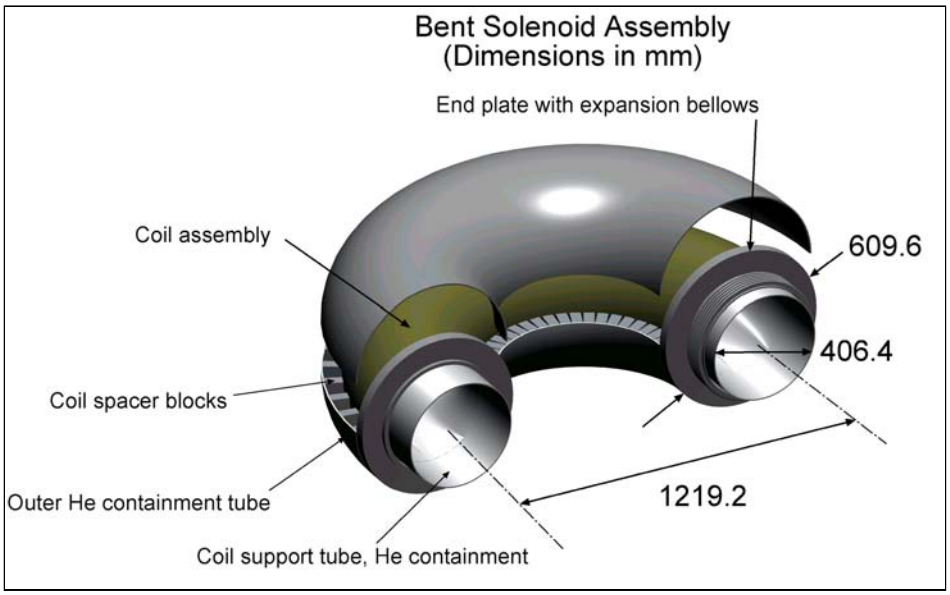

Figure 26. Bent Solenoid Components.

Modern superconducting accelerator magnets, such as RHIC and the once proposed for the SSC, rely on the use of supercritical helium for cooling the magnet. We have assumed that this technology will be used for this application and have used 20 atmospheres pressure as the design requirement for the helium containment. Thus, this design is adaptable to both the supercritical and the low-pressure helium bath cooling.

The helium containment for the bent solenoid requires rather large (i.e. up to 610 mm diameter) pre-formed shells bent to a small radius. Value engineering is applied to the proposed design in order to minimize the cost by using commercially available component sizes that are consistent with the design requirements. Thus, we have selected standard size tube fitting dimensions for the inner and outer tubes of the vessel. These are available in inch dimensions that closely match metric dimensioning requirements. The inner helium containment tube may be obtainable as a seamless tube fitting in a 300 series stainless steel. However, in the event that a welded tube is used, it will be determined if the effect of the welding seam is a field quality issue for the bent solenoid. If it turns out that the field quality requirements are too stringent for the use of a welded tube, then the grade of the material and the welding procedure may need to be optimized for this application. These same considerations also apply to any warm beam tube that may be inserted in the magnet.

Spacer blocks made of low carbon steel laminations are used to provide precise support of the coil relative to the outer shell. One end of the magnet is fitted with an end plate containing a bellows to allow for differential expansion of the components when cooled to operating temperature.

In addition, good cooling of the coil is mandatory since the coils have to operate under significant energy deposition from stray particle flux. Thus, a composite tube with cooling channels (“cooling tube”) will be used between the inner helium containment tube and the coil. This will serve to intercept heat coming in from the beam tube to the magnet and will also serve as the support tube on which the coil is wound.

2.7 Cold Mass Structural Analysis

The cold mass consists of the coil, its support structure, and the helium containment vessel. The bent solenoid requires a helium containment vessel to provide the necessary cooling environment for the superconducting coils and also act as the main support structure for the magnet. The cold mass will also contain provisions for mounting and aligning this assembly in a cryostat. It is intended that any model magnet constructed in Phase II will be tested at a National Laboratory with suitable facilities for testing and measuring superconducting accelerator magnets.

The structural design of the cold mass is based on the following loading conditions:

a. Internal pressure in the helium containment vessel.
It is assumed that the magnet will operate with a cryogenic system that uses supercritical helium as the cryogen in order to obtain an operating temperature of about 4.4 K. In this case the design operating pressure is 20 atmospheres, based on the peak pressure that can be experienced in such a system.

b. Thermal loading
The stress due to the difference between room temperature and operating temperature should be fairly low once equilibrium has been obtained since most of the materials used in the construction of the cold mass have similar thermal contraction values. However, the transient conditions that exist during cool down could produce rather large thermal stresses in the helium containment vessel because the thermal mass of the inner helium containment tube is much less than that of the rest of the structure. Since the cryogen flows around this tube, it could experience a large temperature drop before the rest of the assembly is cooled down. The vessel therefore has been analyzed for this loading condition and a bellows is used at one end of the cold mass to allow for this difference in contraction during cool down.

c. Lorentz force loading
The Lorentz forces that act on the coil are rather large and consist of an internal magnetic pressure plus a compressive force at the ends of the coil. These forces produce local deformations in the coil and must be taken into consideration in the design of the coil and its support structure.

Since the resultants of all of the Lorentz forces must be in equilibrium, they do not transmit any external forces to the pressure vessel structure. Also, the presence of the coil in the helium containment vessel does not contribute much to the structural rigidity of the assembly. Thus the structural analysis of the coil (under the Lorentz force loading) was considered separately from the structural analysis of the helium containment vessel (under the pressure and thermal loading conditions).

The allowable stress values for the helium containment shell, which also provides structural rigidity for the magnet assembly, are based on Section VIII of the ASME Boiler and Pressure Vessel Code. The requirements for the size and shape of the magnet also dictate the method of construction for the 180º-bent solenoid. The use of commercially available shells for the helium containment is strongly advised as a value engineering provision.

Figure 27 summarizes the components that have been selected for the cold mass. The dimensions used for the structural analysis of the helium containment vessel are shown in Figure 28.

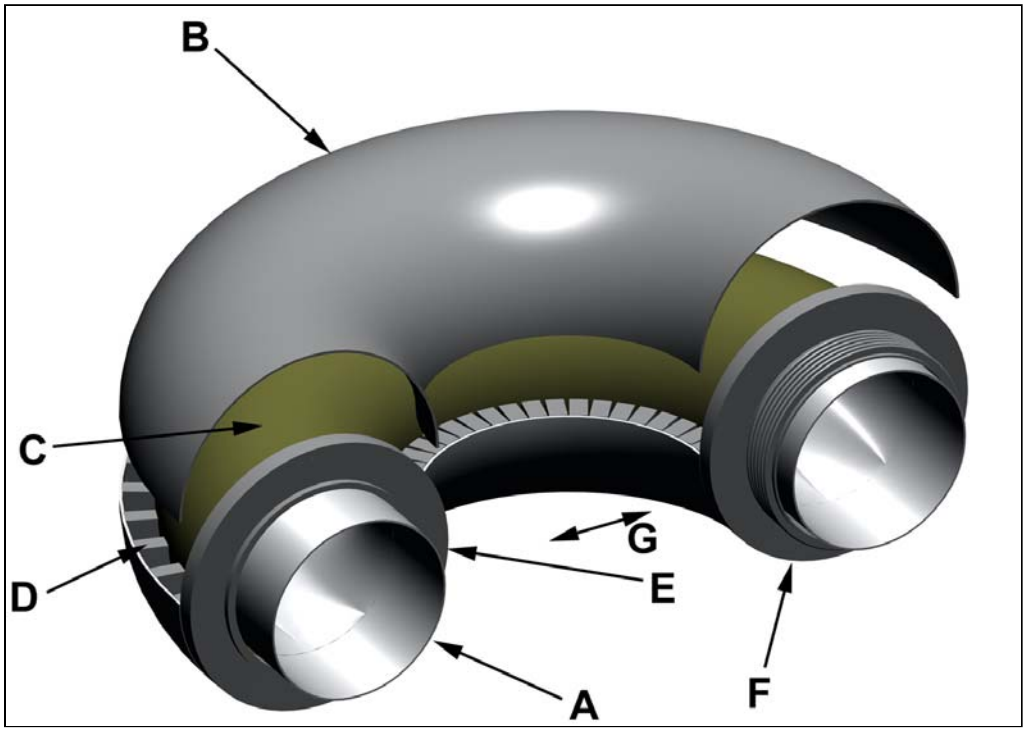

Figure 27. Some components of the cold mass. See Table for legend.

A	Inner helium containment tube (with extensions)	16-inch O. D. (406.4 mm), 0.25-inch wall stainless steel 180º bend tube fitting. Bend radius = 24 inches (609.6 mm). Shown with extensions welded to end of fitting.
B	Outer helium containment shell	24-inch (609.6 mm) O. D. Half shell tube filling, 0.25-inch wall, 180º bend on a 24-inch (609.6-mm) radius.
C	Coil assembly	
D	Support spacers	Laminated steel spacer blocks used to support coil.
E	Helium vessel end plate	End plate welded to inner and outer shells at assembly
F	Helium vessel end plate with bellows.	Welded to inner and outer shells at assembly. Bellows required for reducing thermal load stress.
G	Reinforcing gusset (not shown)	Required for structural reinforcement for pressure load.

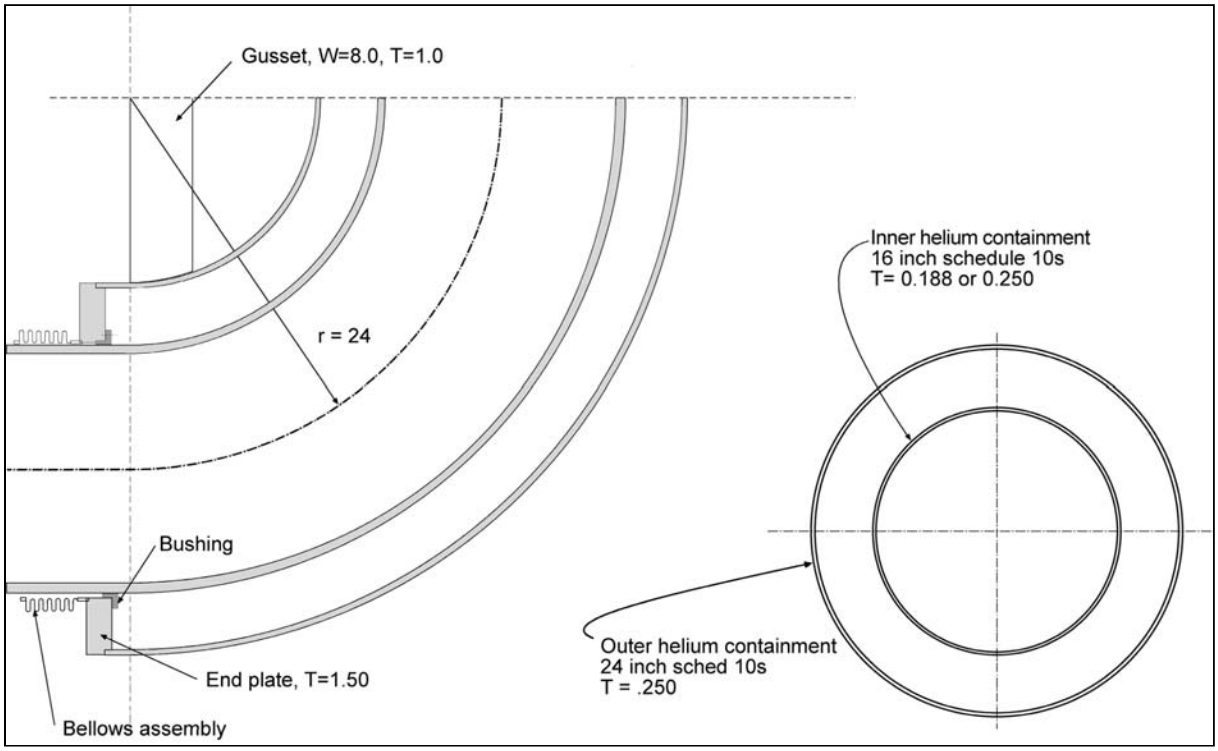

Figure 28. Dimensions used for structural analysis of cold mass.

The finite element structural analysis program ALGOR[5] was used to validate the conceptual designs of the coil and the containment vessel. A complete description of the structural analysis of the coil assembly under the effect of the Lorentz load is contained in a separate report in Appendix I, and the complete description of the structural analysis of the containment vessel is contained in a separate report in Appendix II.

The results of these analyses are summarized here.

a. Helium containment vessel.

The analysis has demonstrated that it is feasible to use a helium containment vessel with a 180-degree bend to house the combined solenoid/dipole magnet. The loading conditions examined included:

- Pressure at 20 atmospheres (300 psi) between the inner and outer vessel for use in a cryogenic system with supercritical helium.
- A temperature load when the inner tube cools to 4.2 K prior to the remainder of the structure.

The possibility that the inner tube cools down much faster than the outer tube required the examination of two possible configurations for this vessel. Configuration 1 allows a virtually unconstrained contraction of the inner tube; a bellows is used to connect the inner tube to one end plate and the other end of the inner tube is welded directly to its end plate with some sort of transition ring. In Configuration 2, both ends of the inner tube are welded to their end plates. (See Figures 29 and 30)

For the pressure load, the result is about the same for both configurations. The reinforcing gusset between the two ends has been found to be a necessary addition for this loading condition. The maximum primary stress in the shells is within allowable limits of the ASME code. There are localized high stresses in the regions between the inner tube and the end plate at the welded end. This stress distribution depends on the detailed de-

[5] ALGOR Finite Element Analysis Software, ALGOR, Inc. 150 Beta Drive, Pittsburgh, PA 15238 USA

sign of the transition weld ring between these two parts. This issue will be treated in Phase II when the detailed design of the vessel is worked out.

If it is proposed to use bath cooling in liquid helium at atmospheric pressure, the pressure load becomes negligible. However, the construction of the vessel would be essentially the same (except perhaps for the elimination of the reinforcing gusset) since the bent tubes require a wall thickness of the order of 0.25 inch in order to be fabricated properly.

If the application for this vessel involves the temperature load on the inner tube, then it appears necessary to use the bellows at one end of the inner tube. Without the bellows, the combined load for this case would produce stresses in the inner tube above the (room temperature) yield point of the material. It is probably good practice not to exceed this value even though at 4.2 K the yield point is about twice the room temperature value.

The reinforcing gusset also appears to have high-localized stress, which arises from the bending of the structure due to the pressure load. The gusset section used in this model is 1-inch thick by 8 –inches wide. A more detailed analysis will be carried out in Phase II to determine the best configuration for this component.

Finally, the method of support of the helium containment vessel in the cryostat assembly needs to be determined as a Phase II activity. It is quite possible that the reinforcing gusset will be part of the assembly that connects to the support and thus the final design of this part will be undertaken at that time.

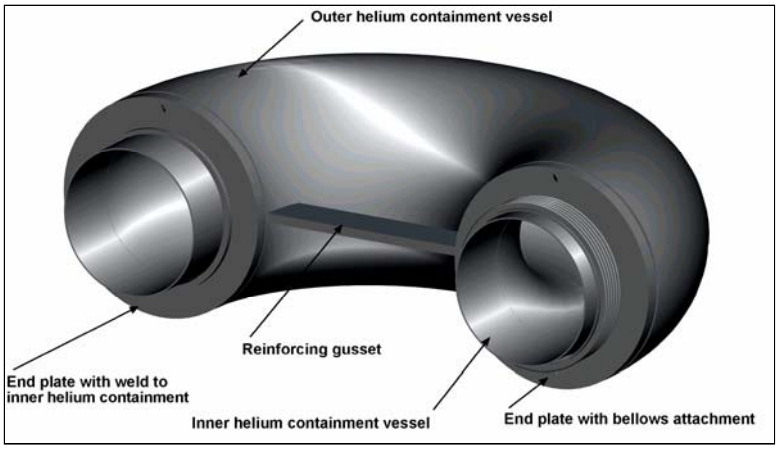

Figure 29. Helium containment configuration with bellows.

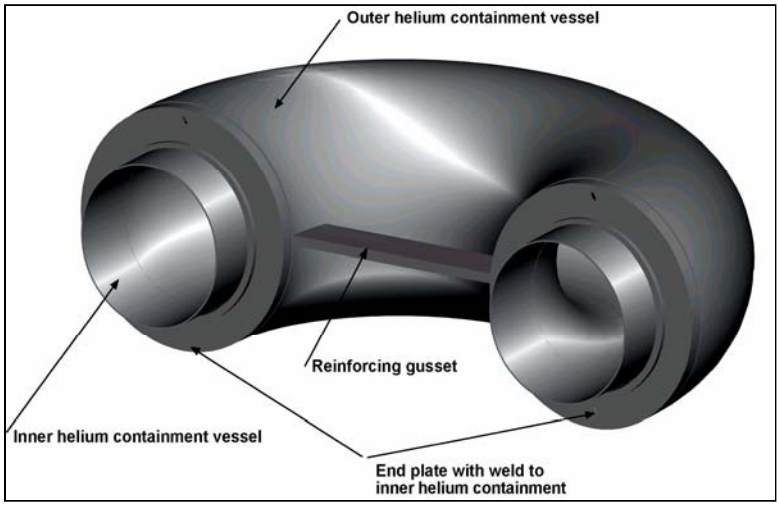

Figure 30- Helium containment configuration with welded end plates at both ends.

b. Coil assembly.

The method of calculating the internal magnetic pressure and coil end forces due to the Lorentz forces is given in Appendix I, which contains the detailed structural analysis, report for the effect of Lorentz loading on the coils. It is seen that the magnetic field within the bent solenoid produces a rather large magnetic pressure on the coils.

The 180° bent solenoid can be considered as half of a toroidal magnet. For a toroidal magnet the magnetic pressure varies from one side of the torus to the other because the field seen by the coils is stronger on the inner side of the torus than on the outer side. In this case the magnetic pressure at the inner radius is about 1.40×10^7 N/m^2 (~2037 psi) and at the outer radius it drops to 3.51×10^6 N/m^2 (~509 psi). The value at the mid radius is that for the straight solenoid, 6.24×10^6 N/m^2 (~905 psi).

The analysis has shown that a coil assembly can be designed such that the relatively large Lorentz loading produced by a nominal field of 4 tesla in the magnet will produce relatively low deflections and stresses in the coil. This was demonstrated with a composite coil of 1-inch thickness, supported with spacer laminations and the external helium containment shell. For comparison, the table shows deflections and maximum stress values for coils of thickness 0.5 inches and 1- inch. Although the thickness of the coil may be optimized in a more detailed analysis in Phase II, this analysis has shown that the design is structurally adequate to avoid quench initiation in a real magnet.

	1-inch thick coil	0.50-inch thick coil
Maximum deflection	23 mils	40 mils
Maximum princ. stress	3100 psi	11,000 psi

2.8 Coil Winding Machine

A detailed design, fabrication and test of a 1/3-scale prototype-winding machine was completed in Phase I. The original plan was to build a table-top winding fixture to study the winding process of bent solenoids with tilted winding planes. Due to AML's expertise and existing technology for automated winding, the AML expanded this work and completed a two axis automated winding system for solenoids with a radius of approximately 1/3 meter. This effort was very valuable and will allow us to build a full-scale winding system with minimal design and risk.

The prototype-winding machine with its control system is shown in Figure 31 and a close-up of the winding mechanism is shown in Figure 32. A titlted plane single layer coil wound on this machine is shown in Figure 33.

Figure 31. One-third scale model of machining and coil winding machine for the bent solenoid coil

Machine Configuration Overview

The full-scale system will accommodate bent solenoids with a radius of 1 meter and a winding support tube of 500 mm diameter. In addition, it will require two more axes of automated control and scaled up mechanics. Key features include:

- 4-axis of coordinated motion control
- Axis 1 – Horizontal rotation of solenoid
- Axis 2 – Orbital rotation of routing and winding around solenoid
- Axis 3 – Linear movement perpendicular to axis 2 to control routing and winding position
- Axis 4 – Wire feeding/tension control
- Electrical slip ring

- Adjustable tilt angle of orbiting axis from 0° to 35°
- Software
- CoilCAD™ coil/magnet design software
- RoboWire™ control software

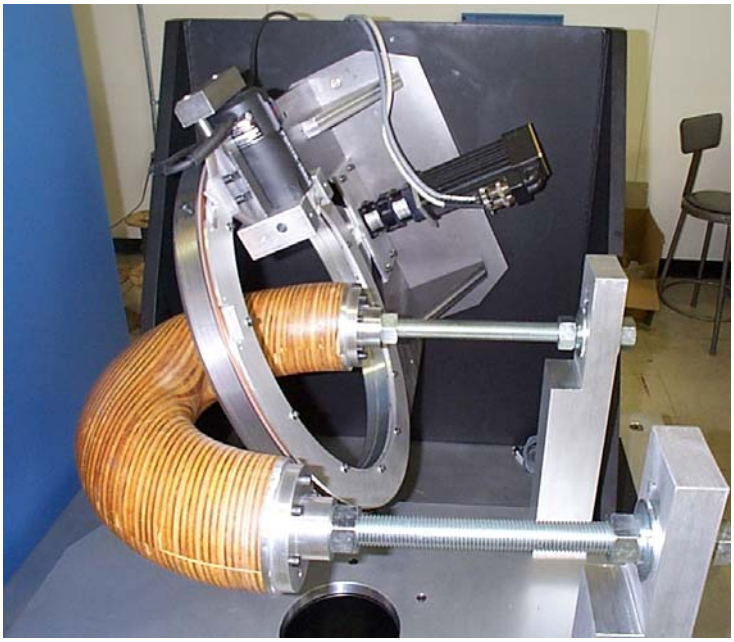

Figure 32. Close-up view of winding machine with 1/3-scale bent solenoid model

Theory of Operations

The bent support tube is mounted at its two ends with large machine chucks. Additional steady rest supports, which were not necessary for the 1/3-scale model, will be added. The mounted tube can rotate around the solenoid vertical Z-axis. A winding end effector, which positions and tensions the conductor, is mounted to a circular support structure. The end effector orbits along the path defined by this support structure (solenoid A-axis). The support structure itself is stationary, but the plane of the orbit relative to the bent tube is adjustable.

Routing and winding proceed in the following way: The orbit plane of the end effector is adjusted to the required angle. While the bent tube rotates around the Z-axis, the end effector orbits around the A-axis. An additional axis controls the depth of routing and winding into the tube. Servo control keeps the movement of all axes coordinated; their relative speed defines the angular advance of the solenoid around the support tube.

Before coil winding, the AML winding machines are also used for machining support grooves for the conductor. For this purpose a high-speed router is mounted in place of the winding end effector. Machining on the winding machine is not only cost-effective, but has several other advantages. The coil support tube is only aligned at one time, and the same coordinate file that controls the end effector movement is used. The coordinate file is generated by AML's CoilCAD™ software. RoboWire™ software, also developed by AML, provides the graphical interface and process control.

It is planned to separate the layers of the solenoid by thin fiber-reinforced over wraps that can be machined with the groove pattern for the next layer. This would improve the conductor placement accuracy for tilted planes during the winding process and would give additional stability to the coil. After the winding of the coil is finished, it is over wrapped with epoxy impregnated fiber-reinforced material. This way the coil is fully en-

capsulated to achieve maximum strength and to prevent any conductor movement under the effect of Lorentz forces, which might quench the magnet.

If it is necessary for any reason to wind a cosθ coil (e.g., dipole or quadrupole) over the finished solenoidal coil, AML has the technology to produce these coils. A robotic arm could be equipped with an AML winding end effector to wind saddle-shaped coils on top of the finished bent solenoid.

Figure 33. Single layer, tilted plane coil wound on model winding machine.

2.9 Magnet Final Assembly

Figure 34 illustrates the assembly and welding sequence for the bent solenoid. Subsequently the external electrical assembly of the power and instrumentation leads are completed. The magnet will then be put though a series of tests and measurements to obtain electrical and mechanical data such as:

- Hipot verification of insulation integrity
- Resistance measurement of coil
- Dimensional mechanical measurements
- Verification of helium containment integrity with a mass spectrometer leak detector

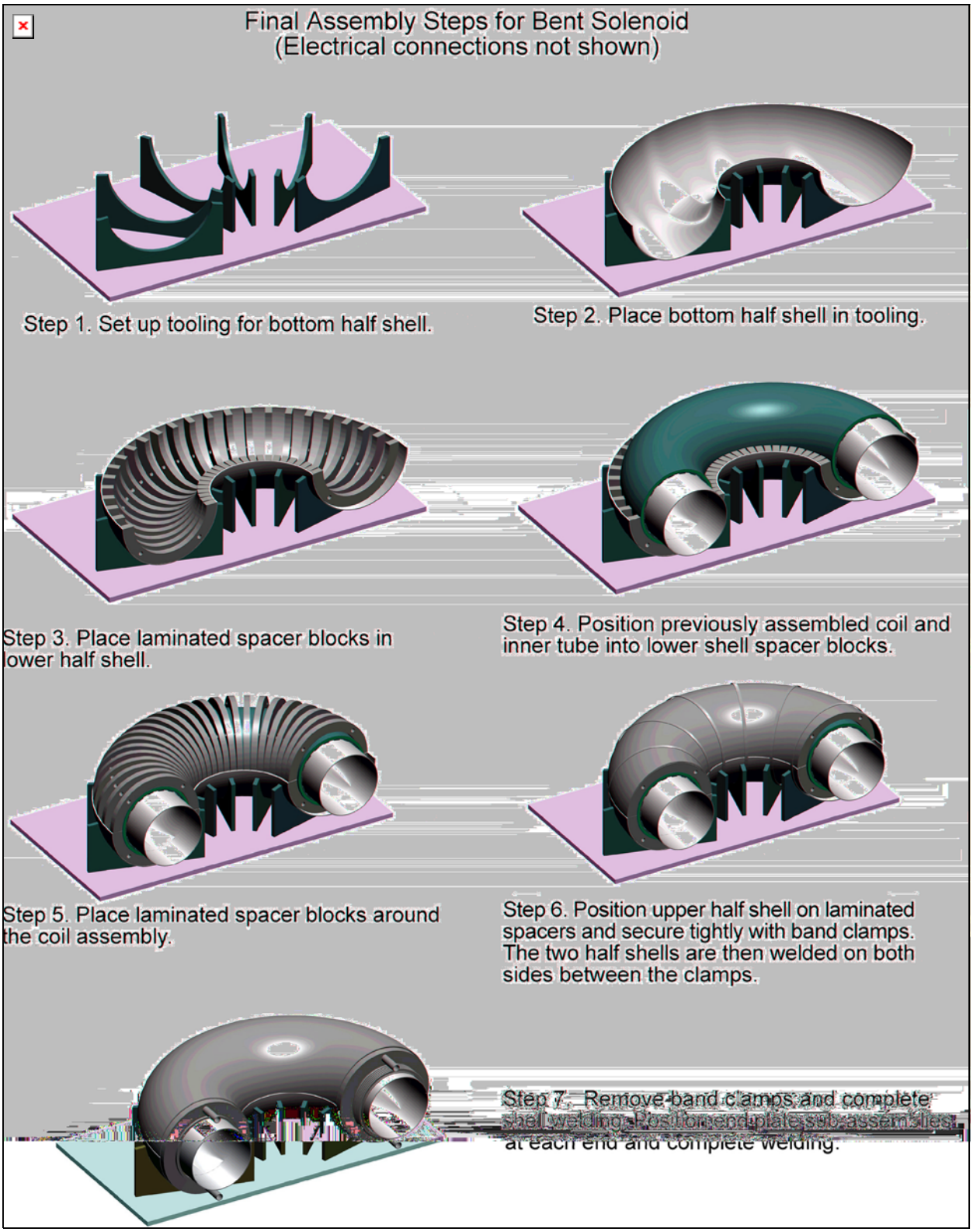

Figure 34. Final Assembly Steps

3. RESULTS: DESIGN PARAMETERS

Based on the magnet parameters set forth in the SBIR solicitation, we have developed a conceptual design for a 180º-bent solenoid with a superimposed dipole field. This magnet has a nominal central field of 4 tesla with a superimposed dipole field of 1 tesla. The coil aperture has been chosen to be 416.6 mm assuming that a warm beam tube of about 300 mm diameter would be used in the magnet. However, if the application does not require a warm beam tube, but rather the cold beam tube style used in RHIC and other accelerators, the coil aperture could be reduced in order to provide a less expensive option.

The basic components of the cold mass are shown in magnet cross section, Figure 35.

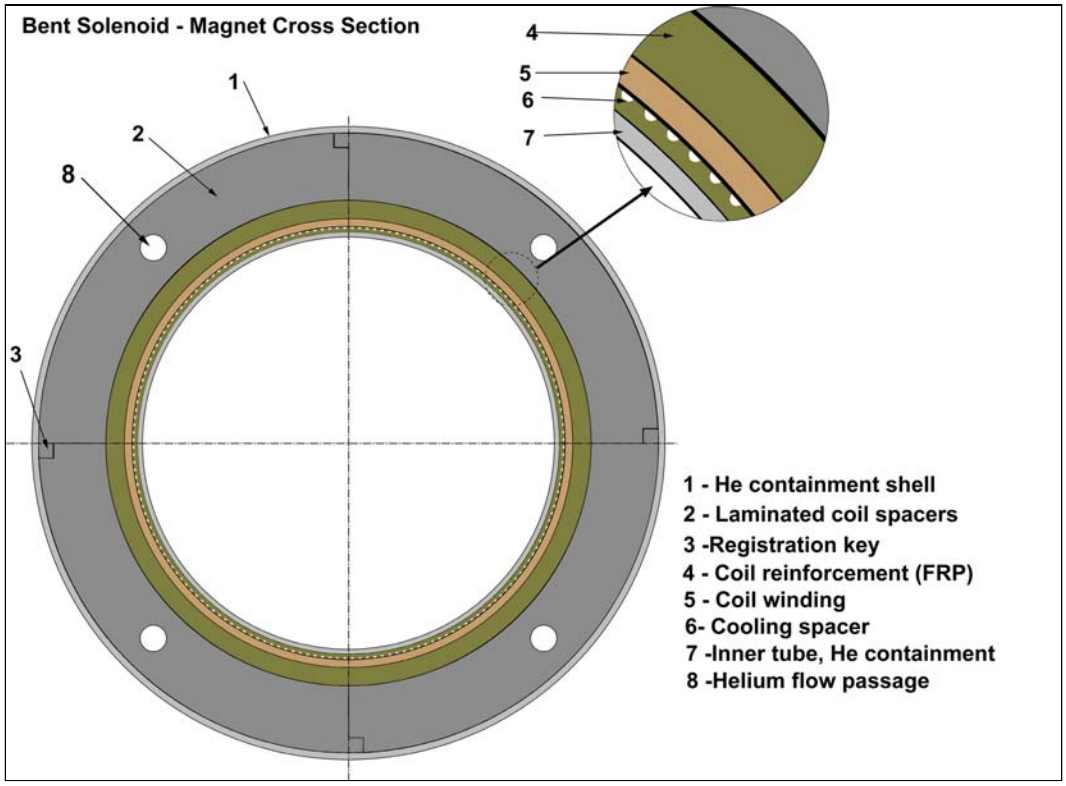

Figure 35. Cross Section of Cold Mass

The bend radius of the magnet has been chosen to be 609.6 mm because the formed shells required for the helium containment vessel are available in a standard bend radius of 24 inches. Any departure from this dimension would require custom-formed shells at a rather large increase in price.

The parameters for the magnet are shown in the following tables.

Table 3.1. Basic Parameters

Magnetic length along axis	1915 mm
Coil aperture	416,4 mm
Solenoid field along axis	4 T
Dipole field on axis	1 T
Quench field along axis	5 T
Operating current	1440 A

Operating temperature	< 4.6 K
Inductance	1.42 H
Stored energy	1.47 MJ
Max field on conductor	6 T
Operating margin at 4.6 K	25%
Cold mass weight	360 kg

Superconducting wire and cable properties

Table 3.2 Wire (Strand) Properties

NbTi composition (%Ti)	47.0
Critical parameter condition	4.23 K and 6T
Critical current, A	61.7
J_c, A/mm^2	2500
Cu/Superconductor	2.35
Strand dia, mm	0.32
Filament dia., μ	9.8
Cu RRR	38

Table 3.3. Cable Properties

Strands/cable	37
Critical current, A	2282
Cable diameter (bare), mm	2.35
Cable insulation	Kapton
Cable dia. (insulated), mm	2.45

Coil Parameters

Figure 34 shows a cross section of the conductor layout in the coil winding. Six layers are used to produce a nominal field of 4 T along the axis of the bent solenoid.

Table 3.4 Coil Parameters

Number of layers	6
Total number of turns	4256
Inner radius, mm	208.2
Outer radius, mm	226.2
Winding plane tilt	25º
Coil winding pitch, mm	2.70
Layer thickness, mm	3.0
Conductor length, m	5808
Conductor mass, kg	143

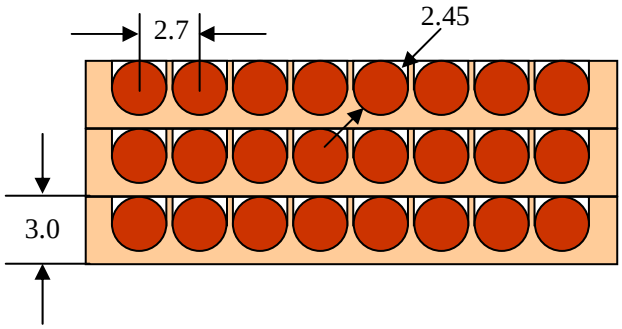

Figure 36. Geometrical pattern of coil cross section showing conductors supported in machined U-grooves. Only 3 out of 6 layers shown

4. TECHNICAL FEASIBILITY

4.1. Magnetic design

The basic requirements for the magnetic design of the bent solenoid were quite general; i.e. 3 – 5 tesla solenoid field with a superimposed dipole field of ~ 1 tesla. This requirement has been met with the design presented herein.

Detailed magnetic field calculations were performed during Phase I and as a result a coil using tilted winding planes has been developed which produces the required combined field. These calculations have also included a precise description of the magnetic field including the significant multipoles present in the field along the length of the magnet as described in Section 2.3.

Although liaison work with the Muon collider group has been very valuable during the execution of this phase of the effort, the field quality requirements for the final application of this magnet have yet to be developed. Thus, the coil design needs to be evaluated with respect to any forthcoming field quality requirements. It has been suggested that the field quality requirements for this application are rather modest.

4.2. Operational considerations

Quench protection issues:

The use of the selected cable for the magnet provides an operating margin of ~25%. The magnet also operates such that the current density on the copper (that could occur during momentary perturbations when the current might be shunted into the copper) is ~700 A/mm^2 which is a comfortable level to provide stability against quenching. Thus we expect stable and reliable operation in service.

Because of the relatively high stored energy and inductance of this magnet, special attention is required for the quench protection of the full sized magnet.

In order to obtain an accurate assessment of the quench protection issue, it will be necessary to do a study of the quench propagation velocity in the magnet coil. It will also be necessary to compute the maximum allowable MIITS that can be absorbed by the cable during the quench in order to limit the hot spot temperature to an acceptable level. This activity is planned for Phase II. Various methods to control the MIITS will be studied, such as:

- Employing an external dump resistor.
- Using resistors at the end of each layer to quickly detect the quench and then shunt the current to the external resistor.

4.3 Radiation Resistance Issues

The principal organic materials used in the construction of the magnet are Kapton cable insulation and composite laminate used in the coil assembly. These are regarded as radiation hard materials. For example, test results of materials irradiated at a temperature of 4 K [6] indicated that Kapton shows only a slight decrease in mechanical properties after a dose of 10^9 rads. Typically, composites such as Permaglass ME 730 and TE630, which were proposed insulating materials, showed little or no change after 10^9 rads at 4 K.

The adhesive systems used for the composite support tube and for structural bonding of the conductors in the coil have to be sufficiently radiation hard for operation in the Muon Collider. Such adhesive systems have been developed in collaboration with Composite Technology Development, Inc. (CTD). CTD has developed and commercialized several epoxy-based insulation materials that are optimized for superconducting magnet applications, with demonstrated performance at cryogenic temperatures. CTD led the fusion effort for the development, screening, and characterization of radiation-resistant insulation and adhesives for the US participation in the ITER program. As part of this effort, CTD carried out an extensive radiation test program in which candidate insulation materials were irradiated at 4 K in the fission reactor at the Technische Universitat Munchen in Garching, Germany.

4.4. Structural design

The helium containment and coil structure has been conservatively designed for a pressure load of 20 atm that could occur with the use of a cryogenic system using supercritical helium. In addition the structure has been provided with a bellows for protection against transient thermal stress due to sudden cooling of the inner helium containment tube. The components for the helium containment structure have been selected using value engineering to achieve the lowest cost consistent with requirements.

4.5 Manufacturing development

The use of the 37-strand cable with the coil winding technique described for this application has been demonstrated to produce an accurate, fully supported coil pattern for the tilted winding plane coil. AML has successfully demonstrated the coil winding technique using a one-third scale model as explained in Section 2.7. Using AML internal funding, this model and the ancillary equipment was developed to a greater extent than described in the Phase I proposal.

A preliminary set of assembly steps for the magnet has been developed and was shown in Section 2.8. It employs welding and assembly procedures that have been successfully employed in the assembly of many accelerator magnets such as SSC dipoles and quadrupoles and RHIC magnets.

4.6 Cryostat Requirements

The final design for this magnet will require a cryostat to isolate the cold mass from the warm environment. Basically this will consist of a low heat leak post to support the magnet cold mass, an 80 K heat shield cooled with liquid nitrogen to surround the cold mass, and a steel vacuum vessel to house these components. In addition, the cryostat must provide access to the cold mass from an external power supply and cryogenic system by means of feed-throughs in the vacuum vessel. Depending on the final configuration, provision has to be made for either a warm or cold bore tube to pass through the cryostat.

[6] A. Spindel, "Report on the Program of 4 K Irradiation of Insulating Materials for the Superconducting Super Collider", Draft of 7/8/93.

The conceptual design of the cryostat for the bent solenoid was not included within the scope of this Phase I effort. However, in Phase II, a 90° arc version of the 180° bend magnet will be constructed. It is planned to provide a simple cryostat to house this demonstration magnet so that it can be tested at a cryogenic test facility at one of the national laboratories.

4.7 Summary

The results of the research in Phase I indicate that the bent solenoid can be manufactured at a reasonable cost and that the design is structurally robust and operationally stable. Furthermore, the design features and construction method can easily be applied to variations of this design that may emerge once additional requirements are developed for the Muon Collider.

Issues that need to be addressed in Phase II include (a) quench protection considerations based on the large amount of stored energy and the relatively large inductance of this magnet and (b) verification of the field quality requirements for any beam dynamics in the magnet.

AML feels confident that both of these issues can be successfully addressed in the next phase and therefore has a high level of confidence in the technical feasibility of this project.

APPENDIX I

BENT SOLENOID COILS[†]
STRUCTURAL ANALYSIS FOR LORENTZ LOADING

Carl L. Goodzeit

1. Foreword

Figure 1 shows the configuration of the coil that is used in this analysis. When the magnetic pressure is applied to this structure, a considerable end force is generated by the magnetic field so that there is no net resultant force on the coil. Although no external forces are transmitted to the pressure vessel structure as a result of the Lorentz forces, these forces tend to produce local deformations in the coil itself and must be taken into consideration in the design of the coil and its support structure. Thus, the structural analysis of the coil with the Lorentz force is considered independently rather than as part of the structural analysis of the helium containment assembly.

2. Model used for analysis

The coil assembly was analyzed using the structural analysis package ALGOR[7]. The finite element model used in this analysis consists of the coil and laminated support spacers as shown in Figure 2.

For structural purposes the coil assembly can be modeled as a fiberglass reinforced laminate tube. The presence of the coil superconductor material is neglected since the major portion of the coil cross section needs to be a structural laminate in order to resist the Lorentz force loading.

The dimensions are the same as those used for the analysis of the helium containment vessel except that the thickness of the composite tube that represents the coil has been increased to 1-inch.

The laminated steel spacers that are placed between the coil assembly and outer tube are modeled with plate elements. The spacers position the coil inside the outer shell and minimize local deformations in the coil from the Lorentz loading.

3. Materials

The coil is modeled with filament wound epoxy fiberglass having orthotropic material properties as listed in the Table. Other components are assumed to be 304 stainless steel.

Elastic modulus, E_n	3.5e6 psi
Elastic modulus, E_s	3.5e6 psi
Shear modulus, G_{ns}	1.0e6 psi
Strain ratio, ν_{ns}	0.15

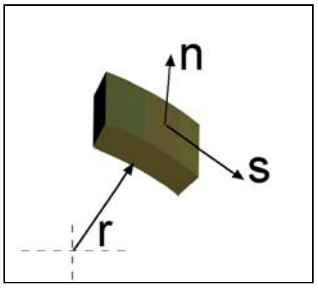

[†] Work supported by U.S. Dept. of Energy SBIR grant DE-FG02-99ER82730
[7] ALGOR Finite Element Analysis Software, ALGOR, Inc. 150 Beta Drive, Pittsburgh, PA 15238 USA

4. Analysis and Results

a. Loading condition

The distribution of the internal magnetic pressure produced by the Lorentz forces on the coil at an average field of 4 tesla was computed as shown in Appendix I-A and is shown in Figure 3 as a function of the angle from the center plane at the outer side of the torus.

For the purpose of structural analysis, it is sufficient to use the average pressure acting on the outer half of the bent solenoid and that acting on the inner half. It is assumed that this pressure remains constant along the length of the coil and thus does not decrease near the ends. Thus, the loading condition is slightly higher than in the real magnet.

The average pressure values[8] shown were applied to the inner (1561 psi) and outer (635 psi) segments of the bent solenoid. This pressure distribution required a compressive end force of 136,260 lbs. for equilibrium. Thus, the two pressures and the end force constitute the Lorentz force loading condition for the coil.

b. Structural analysis results.

The deflected shape of the coil with the Lorentz force loading is shown in Figure 4. It is seen that the coil compresses along its length with maximum compression of 23 mils at the end. The shape of the coil is held circular by the support structure. It is also noted that the stress levels in the coil are reasonably low.

5. Conclusions

The analysis has shown that a coil assembly can be designed such that the relatively large Lorentz loading produced by a nominal field of 4 tesla in the magnet will produce relatively low deflections and stresses in the coil. This was demonstrated with a composite coil of 1-inch thickness, supported with spacer laminations and the external helium containment shell. For comparison, the table shows deflections and maximum stress values for coils of thickness 0.5 inches and 1- inch. Although the thickness of the coil may be optimized in a more detailed analysis in Phase II, this analysis has shown that the design is structurally adequate to avoid quench initiation in a real magnet.

	1-INCH THICK COIL	0.50-INCH THICK COIL
MAXIMUM DEFLECTION	23 MILS	40 MILS
MAXIMUM PRINC. STRESS	3100 PSI	11,000 PSI

[8] English units are used as a matter of convenience for component selection and structural analysis interpretation.

Figure 1: Diagram of coil with support.

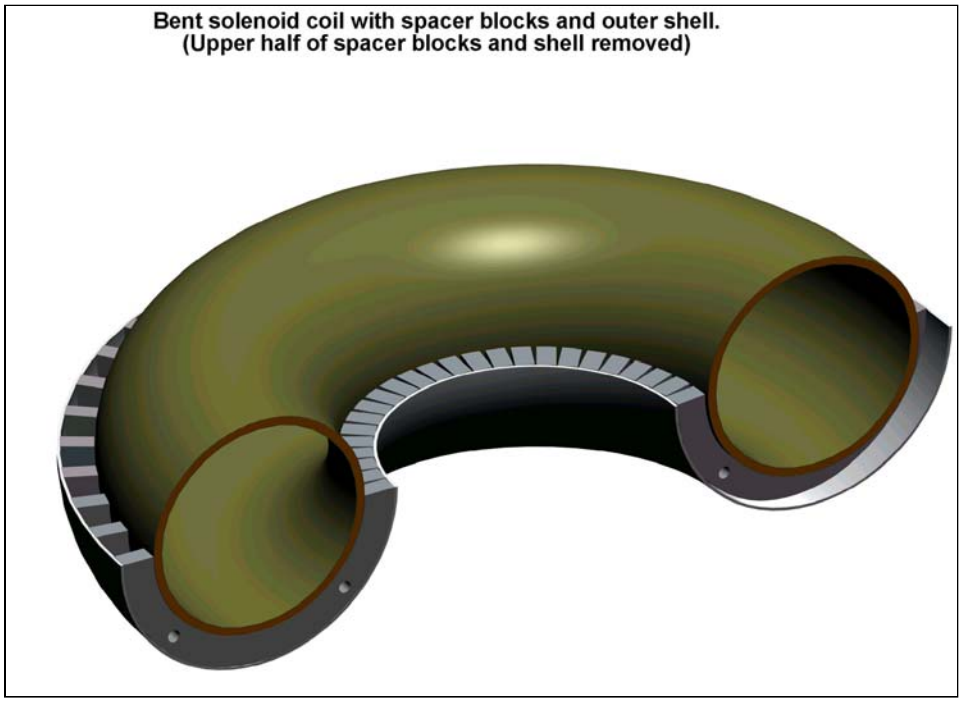

Figure 2: Finite element model of coil with supports.

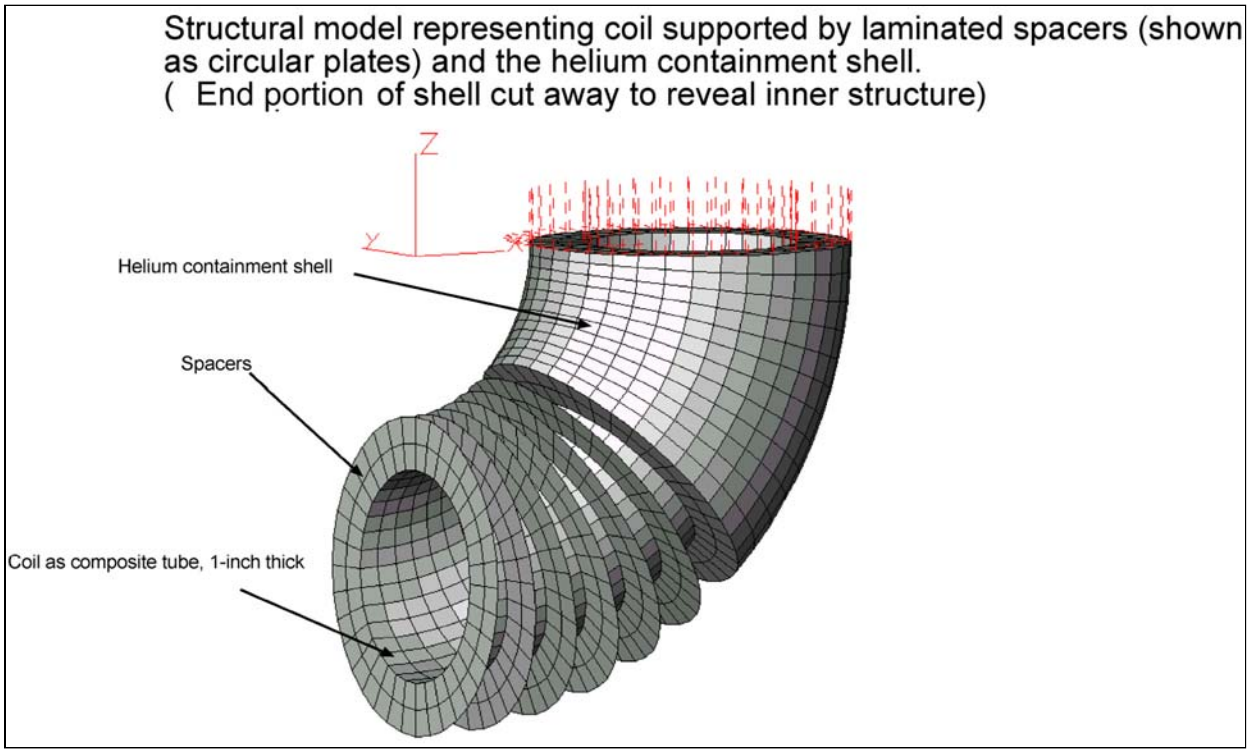

Figure 3: Pressure variation in bent solenoid as a function of angle from the outer side center plane. Average values used for inner and outer halves are indicated.

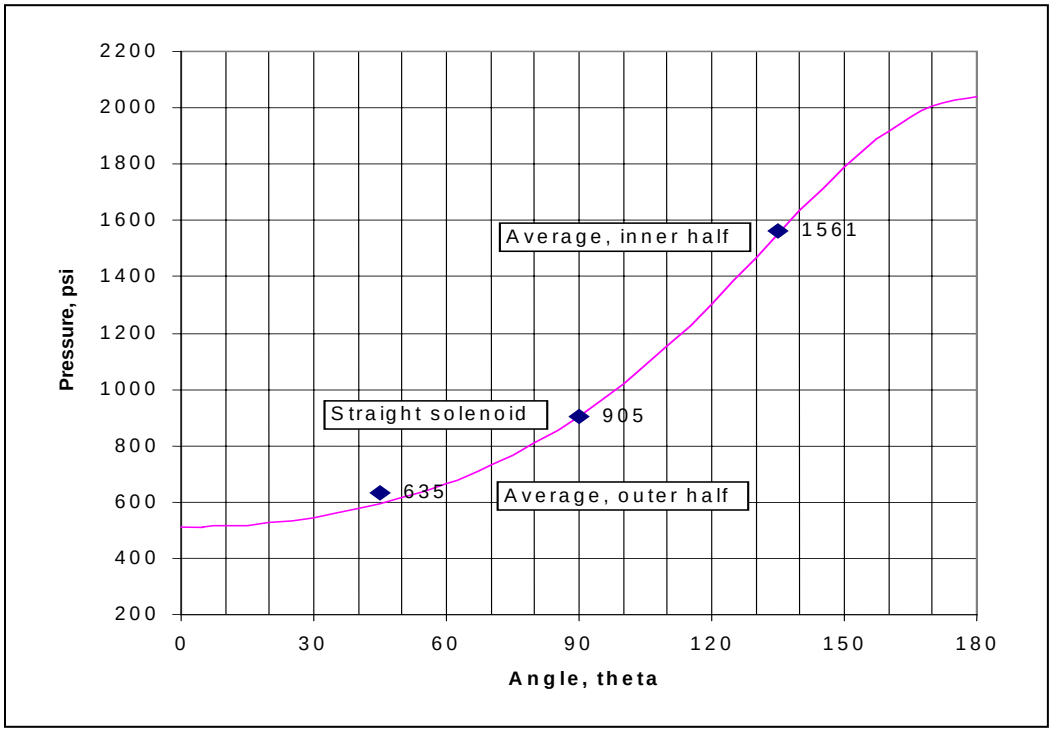

Figure 4. Structural analysis results

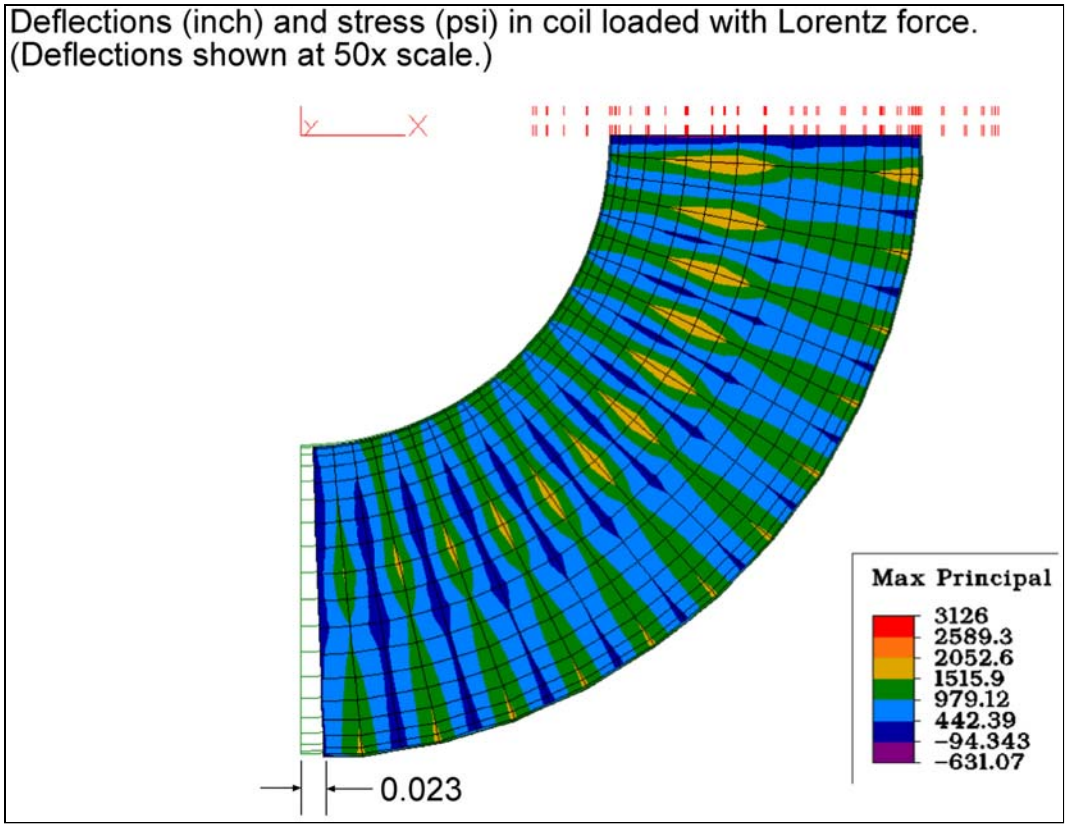

AML Proprietary Information

APPENDIX I-A
FORCE ON A BENT SOLENOID COIL

(Ref. R. Meinke)

An ideal circular-cross-section torus, as shown in the diagram, is energized with a surface current sheet. The surface current occupies zero thickness and flows around the torus perpendicular to the toroidal direction, φ. The current sheet is approximated by N closed current loops, perpendicular to the toroidal direction. The following parameters are consistent with those required to produce a central solenoidal field of 4 tesla in the proposed magnet.

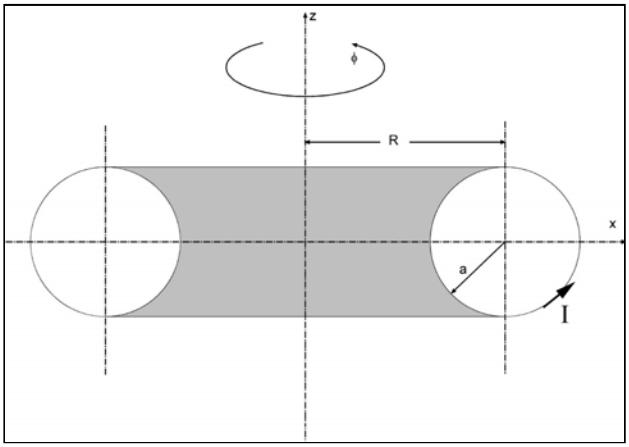

Table A.1

Number of turns, N	2440
Current, I	5000 A
Minor axis, a	203.3 m
Major axis, R	609.6 m

Parameters for 4 tesla torus:

1. The bent solenoid can be considered as a portion of a toroidal magnet where the field along the toroid axis, B_φ, is:

$$B_\varphi = \frac{\mu_0 NI}{2\pi R} = 4.003\ \text{T}$$

Figure A.1 shows a section of the bent solenoid. The horizontal distance from the origin is given by r(θ) +a cos θ. Substituting this into the equation above, it can be shown that on the surface the field varies with the angle, θ:

$$B_\varphi(\theta) = B_\varphi \frac{R}{R + a\cos\theta}$$

It is seen that when R is very large compared to a, the field approaches $B_{\varphi,}$ that which is obtained on the axis of the toroid.

2. Force on the toroidal coil:

Consider the element of area defined by angles dφ and dθ on the surface of the torus as shown in figure A.1. If the arc defined by dφ contains N_{SE} segments of wires of length dl = a dθ, then the radial force acting on the element is:

$$F(\theta) = \frac{N_{SE} B_\varphi(\theta) I dl}{2} = \frac{N_{SE} B_\varphi(\theta) I a d\theta}{2}$$

The factor of ½ is used since the average field seen by the current sheet is B(θ)/2 (i.e. the field is maximum on the inside of the coil and zero on the outside). This force acts on an area defined by:

$$Area(\theta) = ad\theta\,(R + a\cos\theta)d\varphi$$

Thus, the pressure as a function of θ is given by:

$$p(\theta) = \frac{F(\theta)}{Area(\theta)} = \frac{N_{SE}B_{\varphi}(\theta)I}{2(R + a\cos\theta)d\varphi} = \frac{B_{\varphi}N_{SE}IR}{2d\varphi(R + a\cos\theta)^2}$$

Using values for the parameters as listed in Table A.1 we obtain the values for the pressure on the toroidal magnet as shown in Table A.2 and the values are plotted in Figure A.2.

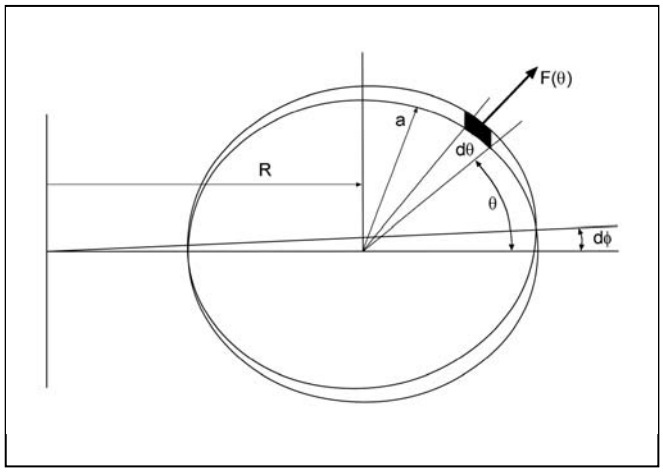

Figure A.1

Table A.2

Angle, θ	Pressure, psi	Angle, θ	Pressure, psi
0	509	95	960
5	510	100	1020
10	513	105	1084
15	518	110	1153
20	525	115	1227
25	534	120	1304
30	545	125	1384
35	559	130	1466
40	574	135	1550
45	593	140	1633
50	614	145	1713
55	638	150	1789
60	665	155	1859
65	695	160	1920
70	729	165	1970
75	767	170	2007
80	809	175	2030
85	855	180	2037
90	905		

Figure A.2

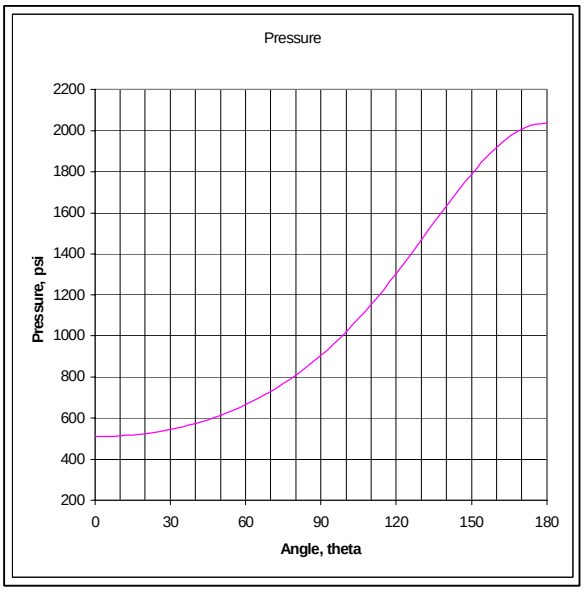

AML Proprietary Information

APPENDIX II

HELIUM CONTAINMENT VESSEL FOR THE BENT SOLENOID[†] STRUCTURAL ANALYSIS

Carl L. Goodzeit

1. Foreword

The bent solenoid requires a helium containment vessel to provide the necessary cooling environment for the superconducting coils and also act as the main support structure for the magnet.

A structural analysis[‡] was performed for two configurations of this vessel. Figure 1[*] shows a view of the first configuration with its component pieces. Note that in this rendition the outer helium containment vessel is attached to the inner one by means of an end plate with a bellows assembly at one end and a welded plate at the other end. In the second configuration, shown in Figure 2, both ends are welded directly to the inner tube. Configuration 2 is applicable if there is no major temperature differential between the inner and outer tubes of the containment vessel.

A reinforcing gusset is used to bridge the two ends of the vessel as shown. This is required since the pressure load causes the vessel to deflect to a larger radius (as in the action of a Bourdon tube).

The magnet coil is contained within this assembly. It is mounted on the inner tube and restrained on the outer surface with spacer laminations held in place by the outer shell as shown in Figure 3. The spacers have holes to allow helium flow through the assembly.

The dimensions of the helium containment assembly used for the analysis are shown in Figure 4.

Value engineering is applied to the proposed design in order to minimize the cost by using commercially available component sizes that are consistent with the design requirements. Thus, we have selected standard pipe size fittings dimensions for the inner and outer tubes of the vessel. These are available in inch dimensions that closely match metric dimensioning requirements.

2. Loading conditions for the Model

The structural analysis presented in this report considers loading conditions that would occur in actual service.

a. The vessel is used in a supercritical helium cooling system with an operating pressure of 20 atmospheres (300 psi).

> Thus, the loading condition is 300-psi external pressure for the inner helium containment tube and 300 psi internal pressure for the outer tube. The end plates are loaded with 300-psi pressure.

b. The rate of cool down is such that the inner tube reaches operating temperature while the rest of the assembly is still at ambient temperature.

> The thermal mass of the coil assembly, spacers, and outer tube is much greater than that of the inner helium tube. Thus, a conservative approach is to assume that the inner helium containment tube cools down much faster than the rest of the assembly. Hence the structure is analyzed for the case of the inner tube at 4.2 K and the rest of the assembly at ambient temperature.

c. The Lorentz forces acting on the magnet coils.

[†] Work supported by U.S. Dept. of Energy SBIR grant DE-FG02-99ER82730

[‡] English units are used throughout this report as a matter of convenience for component selection and structural analysis interpretation.

[*] Figures are shown at the end of the report.

A separate report[9] shows that the Lorentz forces acting on the coil with a central field of 4 tesla produce a very large magnetic internal pressure (average ~ 905 psi) and an end force of about 136,260 lbs. The sum of all of the Lorentz forces acting on the coil are in equilibrium and thus no external forces are transmitted to the pressure vessel structure as a result of the Lorentz forces, per se. However, these forces tend to produce local deformations in the coil and must be taken into consideration in the design of the coil itself and its support structure. Thus, the structural analysis of the coil with the Lorentz force is presented as a separate report.

3. Model used for analysis

The helium containment assembly was analyzed using the structural analysis package ALGOR[10]. Two models were used for the analysis.

Configuration 1 (Figure 1), with a bellows at one end and a fixed plate at the other end, requires a model of the complete 180-degree bend because of this unsymmetrical configuration. The model for Configuration 1 is shown in Figure 5.

Configuration 2 (Figure 2), with both end plates fixed, could be more reliable and less expensive than a bellows assembly and thus is worth examining. This configuration is symmetrical and can be modeled with a 90-degree section. Configuration 2 is modeled using just the upper half of the model shown in Figure 5.

The inner and outer tubes are modeled with plate elements, 0.25 inch thick. The end plates are 1.5-inch thick plate elements and the gusset is 1-inch thick plate elements. The welded connection between the endplate and inner tube is modeled with 3-D brick type elements. However, this section will be examined separately with a more detailed model in the Phase II analysis for the final design of the vessel.

The laminated steel spacers that are placed between the coil assembly and outer tube are modeled with gap elements. These can take only compression and simulate what happens when the inner tube tries to deform in a mode that causes compressive restraint with the outer tube.

4. Materials

Austenitic stainless steel has been chosen for the components of the helium containment vessel because the material welds easily and exhibits excellent mechanical properties at cryogenic temperature. It can be obtained in grades that have a low magnetic permeability (which is important for the inner tube).

We propose the following specifications for the vessel components:

Inner tube: This can be obtained as a standard schedule 10s 180° long radius (24-inch or 0.609 m) return fitting with an outside diameter of 16 inches (0.406 m) and an inside diameter of 0.397 m, which is the design guideline. This can also be obtained in grade 316 LN that, in the annealed form, has a magnetic permeability $\mu \cong 1.008$ at 4K[11]. However, the 16-inch commercially available fitting that is used for this piece is fabricated from two halves that are welded together. The position of the weld is such that it lies precisely on the mid-plane of the superimposed dipole field in the magnet. The increased permeability of the tube due to welds in this geometrical position produces only allowed multipoles in the dipole field. These can be tuned to optimize the magnet design if required to achieve a certain field quality for the dipole.[12]

---

[9] Bent Solenoid Coils: Structural Analysis for Lorentz Loading, Attachment I to Phase I Final Report
[10] ALGOR Finite Element Analysis Software, ALGOR, Inc. 150 Beta Drive, Pittsburgh, PA 15238 USA
[11] K. Nohara, The Status of R&D on High Manganese Austenitic Steels for the Supercollider, ASM-International Materials Week '92 Symposium on High Manganese Austenitic (Stainless) Steels, Nov. 1992, Chicago
[3] R. Gupta, Lawrence Berkeley National Laboratory, Private Communication, August 1999.

Outer shell: Since the magnetic permeability is not an issue, we propose to use grade 304L, which is less expensive. This is a standard 24-inch schedule 10s 180° long radius (24-inch or 0.609 m) return fitting with an outside diameter of 24 inches (0.609 m) and an inside diameter of 0.597 m

Other components: Grade 304L is also suitable.

5. Analysis and Results

Each of the configurations was analyzed in two steps, first for the pressure load and next for the thermal load of the cold inner tube in a warm assembly. The results are summarized here.

a. Pressure load for Configuration 1. (Bellows connection at one end)

The deflected shape of the vessel with a pressure of 300 psi between the inner and outer tubes is shown in Figure 6. The outer tube tends to open up and the inner tube closes up. This causes the bellows to extend by about 0.18 inch. Note that there are also small ripples on the outer tube at its inner radius due to the force applied by the laminated spacers (the gap elements).

The deflections of the inner helium containment tube are shown in Figure 7. The simulation of the spacer blocks with gap elements has provided sufficient constraint for the tube to keep it virtually circular under the pressure loading. The magnet coils are therefore subject to only very small deflections from the pressure loading on the containment vessel.

The stresses produced in the vessel by the 300-psi pressure are shown in Figure 8. The primary membrane stress in the outer tube is about 14,000 psi, which is within the allowable stress limit for the material according to the ASME Boiler and Pressure Vessel Code. Localized areas of high stress are seen at the points where the gap elements that represent the spacer blocks press against the outer shell. These localized stresses would be smoothed out in actual service since the bearing area of the spacer blocks is greater than that represented by the gap elements. There may be some areas of high localized stress around the weld between the end plate and inner tube. An analysis with a refined mesh in that area would be carried out in Phase II to optimize the design.

The inner tube stresses are small compared to the outer tube and are not shown separately.

b. Temperature load for Configuration 1. (Bellows connection at one end)

If we examine the case where the inner tube cools down to liquid helium temperature before the rest of the assembly does, we obtain the deflections shown in Figure 9. The flexibility of the bellows allows the inner tube to retract about 0.23 inch and there is a low stress in the inner tube.

c. Pressure load for Configuration 2. (Welded connections at both ends)

The deflections with 300 psi between the two tubes are shown in Figure 10. Note that the pressure produced a slight bowing of the structure. The resulting stresses are shown in Figure 11 and Figure 12. Except for the region where the end plate is welded to the inner tube, the stresses are similar to those for Configuration 1. The connection between the end plate and inner tube requires a more detailed analysis for the final design and this will be treated in Phase II.

d. Temperature load for Configuration 2. (Welded connections at both ends)

The extreme case of a temperature load where the inner tube cools down before the rest of the structure is used to determine if there is a structural problem when both ends of the inner tube are welded to their end plates.

The deflected shape of the structure under this load is shown in Figure 13. This is to be compared with Figure 9, which shows the deflection for the same load in Configuration 1 (with bellows). With the bellows, the inner tube is allowed to contract by 0.237 inches to a low strain condition in the X direction. However, with both ends welded, the contraction is only 0.052 inches and thus there is considerably more strain in the inner tube for Configuration 2. This results in high forces and significant stress in the inner tube, as shown in Figure 14.

The forces against the rest of the structure due to the contraction of the inner tube produce compressive stress in the outer tube and some bending of the structure (Figure 15).

e. Combined loads

Table I summarizes the combined case of the 300-psi helium pressure and the thermal load on the inner tube. The letters A- E refer to locations in the model that are shown in Figure 16.

The upper portion of the table lists the deflections at A (inner tube) and B (outer tube) in both the X (horizontal) and Z (vertical) directions. These are shown individually for each load and then added to obtain the total effect for each of the two configurations.

Similarly, the lower portion of the table shows the maximum principal stress at typical locations in the gusset (C), inner tube (E) and outer tube (D). It can be seen that the all welded configuration is characterized by having a smaller overall deflection in the structure but a larger strain and stress in the inner tube for both the combined loads and for the temperature load acting alone.

The significance of these results is discussed in the Conclusions section.

Table I

		Configuration 1 (Bellows)		Configuration 2 (Welded)			
Load		A	B	A	B		
Pressure	X-deflection	-0.041	0.138	0.026	0.055		
Pressure	Z-deflection	0.052	-0.022	-0.016	-0.013		
Temperature	X-deflection	0.237	-0.006	0.104	0.052		
Temperature	Z-deflection	0.033	0.004	0.000	0.000		
Total	X-deflection	0.196	0.132	0.130	0.107		
Total	Z-deflection	0.085	-0.018	-0.016	-0.013		
		Configuration 1 (Bellows)			Configuration 2 (Welded)		
		C	D	E	C	D	E
Pressure	Max principal Stress	30500	16400	-12000	30000	13600	-800
Temperature	Max principal Stress	1000	0	5600	20000	-500	18500
Total	Max principal Stress	31500	16400	-6400	50000	13100	17700

6. Conclusions

The analysis has demonstrated that it is feasible to use a helium containment vessel with a 180-degree bend to house the combined solenoid/dipole magnet. The loading conditions examined included:

1. Pressure at 20 atmospheres (300 psi) between the inner and outer vessel for use in a cryogenic system with supercritical helium.

2. A temperature load when the inner tube cools to 4.2 K prior to the remainder of the structure.

The possibility that the inner tube cools down much faster than the outer tube requires the examination of two possible configurations for this vessel. Configuration 1 allows a virtually unconstrained contraction of the inner tube; a bellows is used to connect the inner tube to the end plate at one end and the other end of the inner tube is welded directly to the end plate with some sort of transition ring. In Configuration 2, both ends of the inner tube are welded to the end plate. (See Figures 1 and 2)

For the pressure load, the result is about the same for both configurations. The reinforcing gusset has been found to be a necessary addition for this loading condition. The maximum primary stress in the shells is within allowable limits of the ASME code. There are localized high stresses in the regions between the inner tube and the end plate at the welded end. This stress distribution depends on the detailed design of the transition weld ring between these two parts. This issue will be treated in Phase II when the detailed design of the vessel is worked out.

If it is proposed to use bath cooling in liquid helium at atmospheric pressure, the pressure load becomes negligible. However, the construction of the vessel would be essentially the same (except perhaps for the elimination of the reinforcing gusset) since the bent tubes require a wall thickness of the order of 0.25 inch in order to be fabricated properly.

If the application for this vessel involves the temperature load on the inner tube, then it appears necessary to use the bellows at one end of the inner tube. Without the bellows, the combined load for this case would produce stresses in the inner tube above the (room temperature) yield point of the material. It is probably good practice not to exceed this value even though at 4.2 K the yield point is about twice the room temperature value.

The reinforcing gusset also appears to have high localized stress, which arises from the bending of the structure due to the pressure load. The gusset section used in this model is 1-inch thick by 8 –inches wide. A more detailed analysis will be carried out in Phase II to determine the best configuration for this component.

Finally, the method of support of the helium containment vessel in the cryostat assembly needs to be determined as a Phase II activity. It is quite possible that the reinforcing gusset will be part of the assembly that connects to the support and thus the final design of this part will be undertaken at that time.

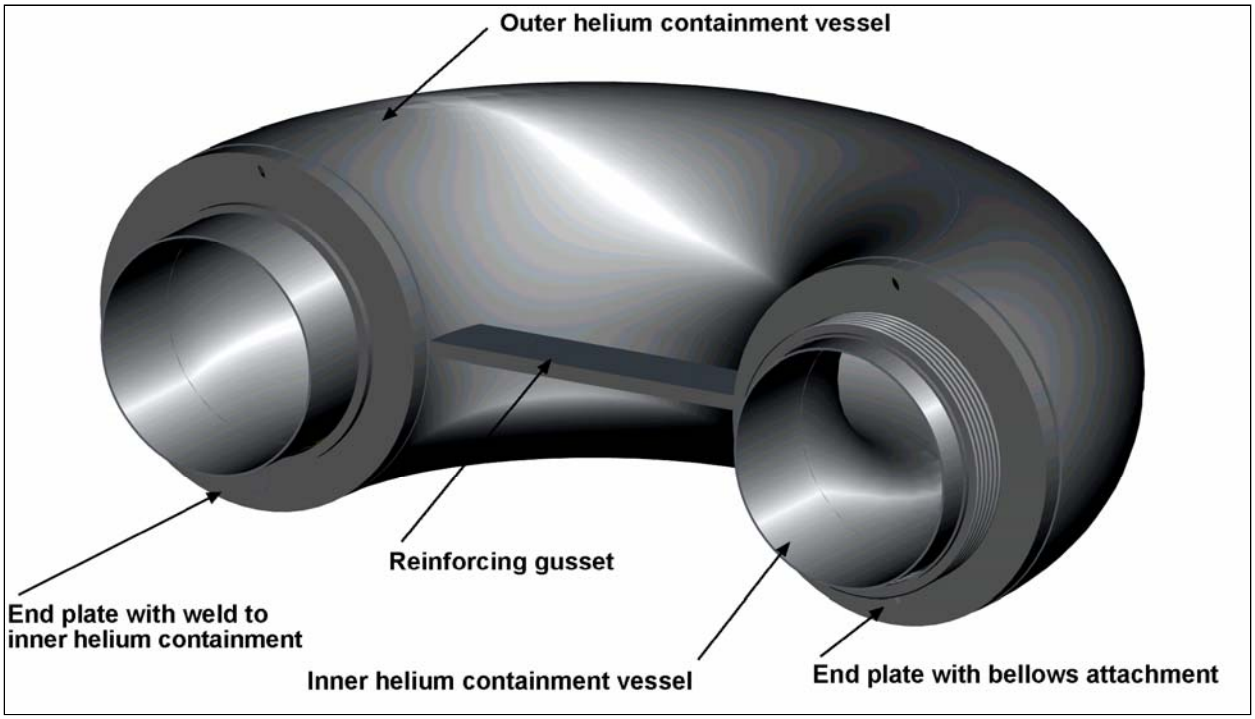

Figure 1. Helium containment configuration with bellows.

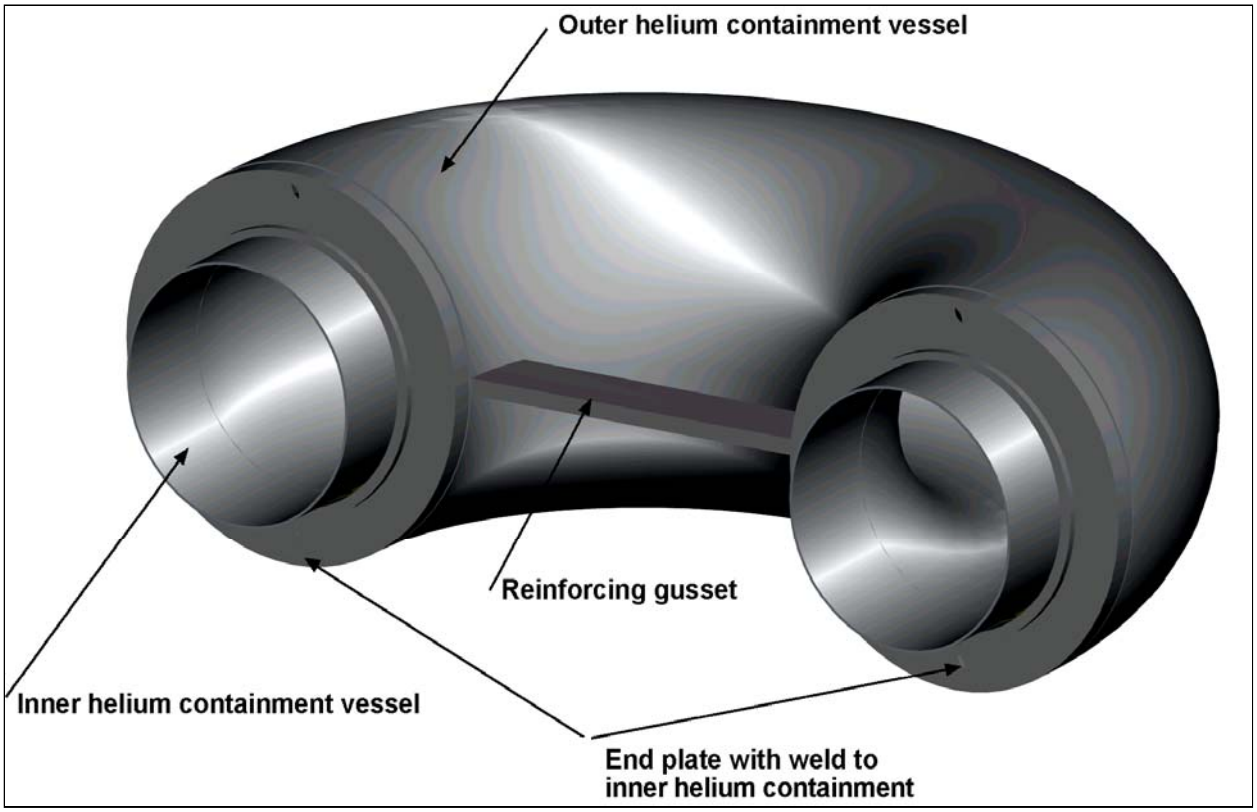

Figure 2- Helium containment configuration with welded end plates at both ends.

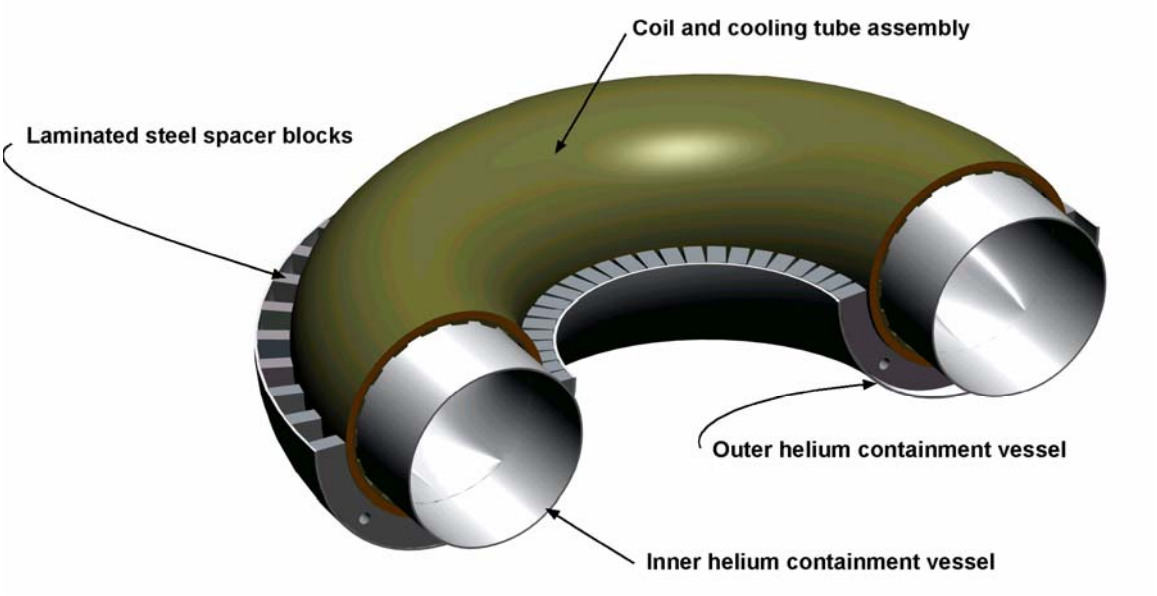

Figure 3 – Section of magnet assembly

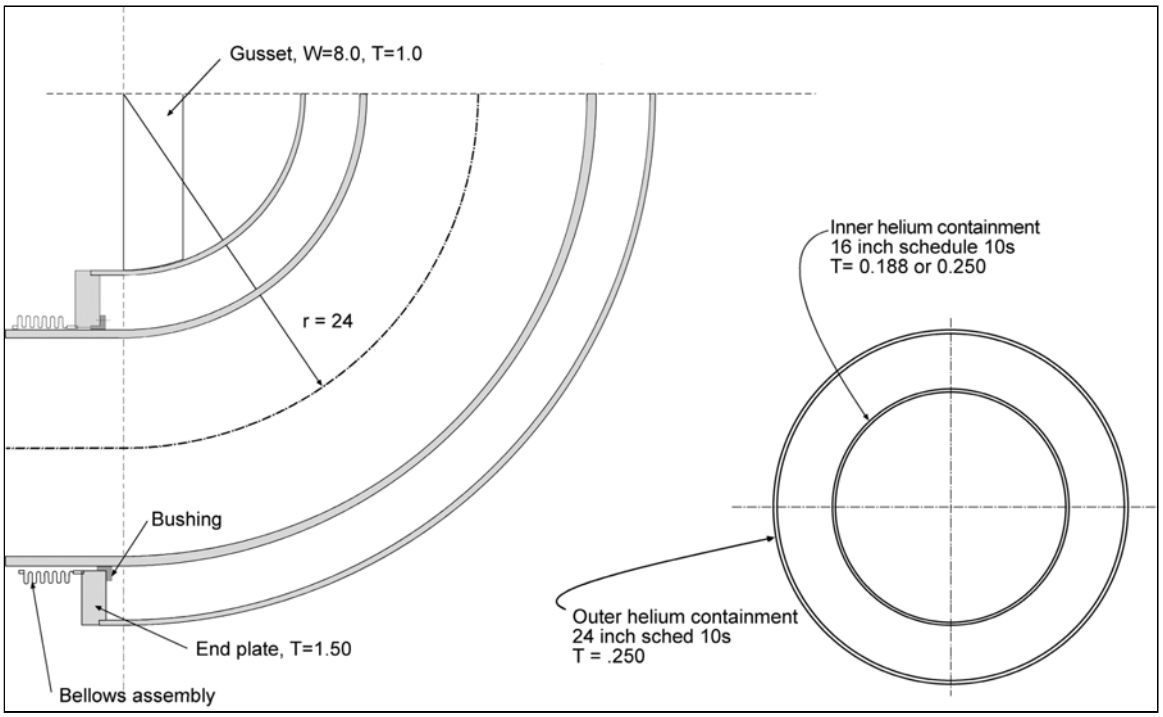

Figure 4 – Principal dimensions of helium vessel (inches).

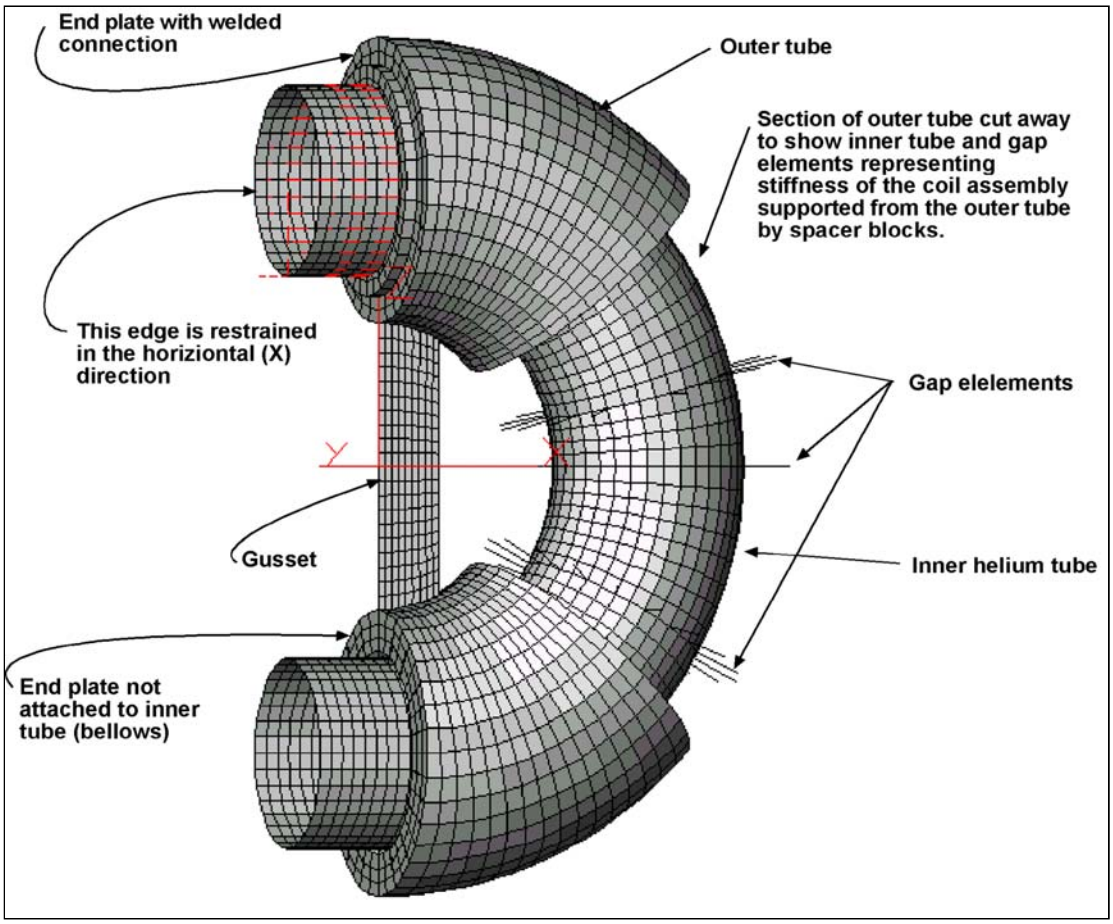

Figure 5 – Finite element model of helium vessel.

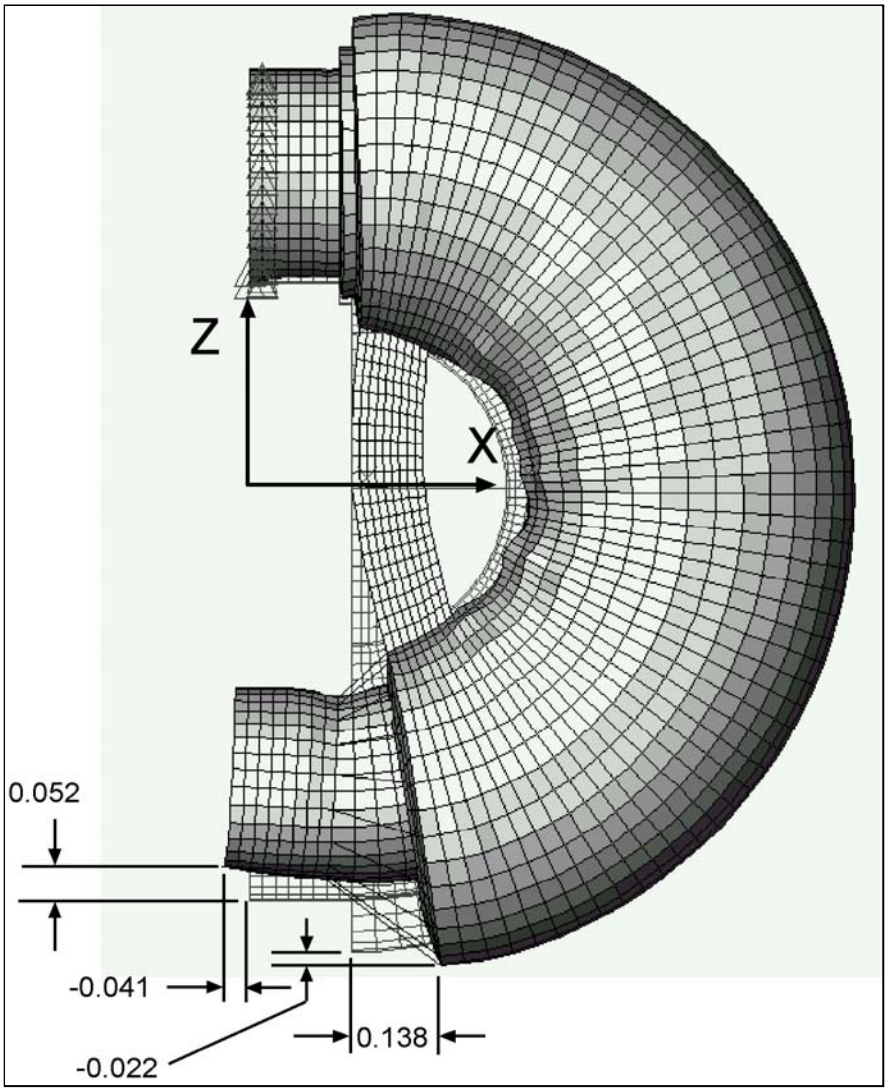

Figure 6 – Configuration 1 deflections with a pressure of 300 psi between the inner and outer tubes. Deflections are magnified by a factor of 50.

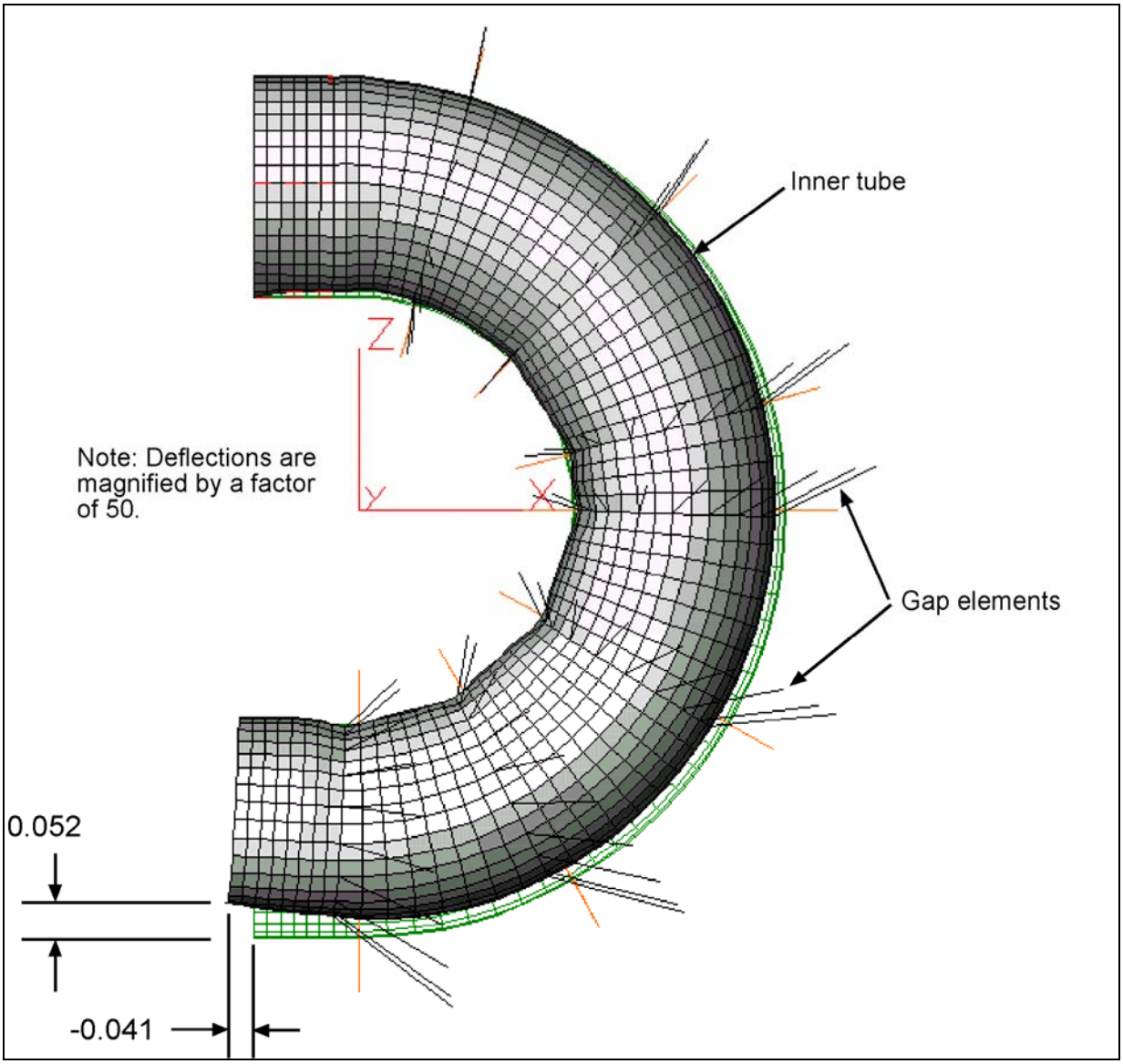

Figure 7 – Deflection in Configuration 1 inner tube due to 300-psi pressure.

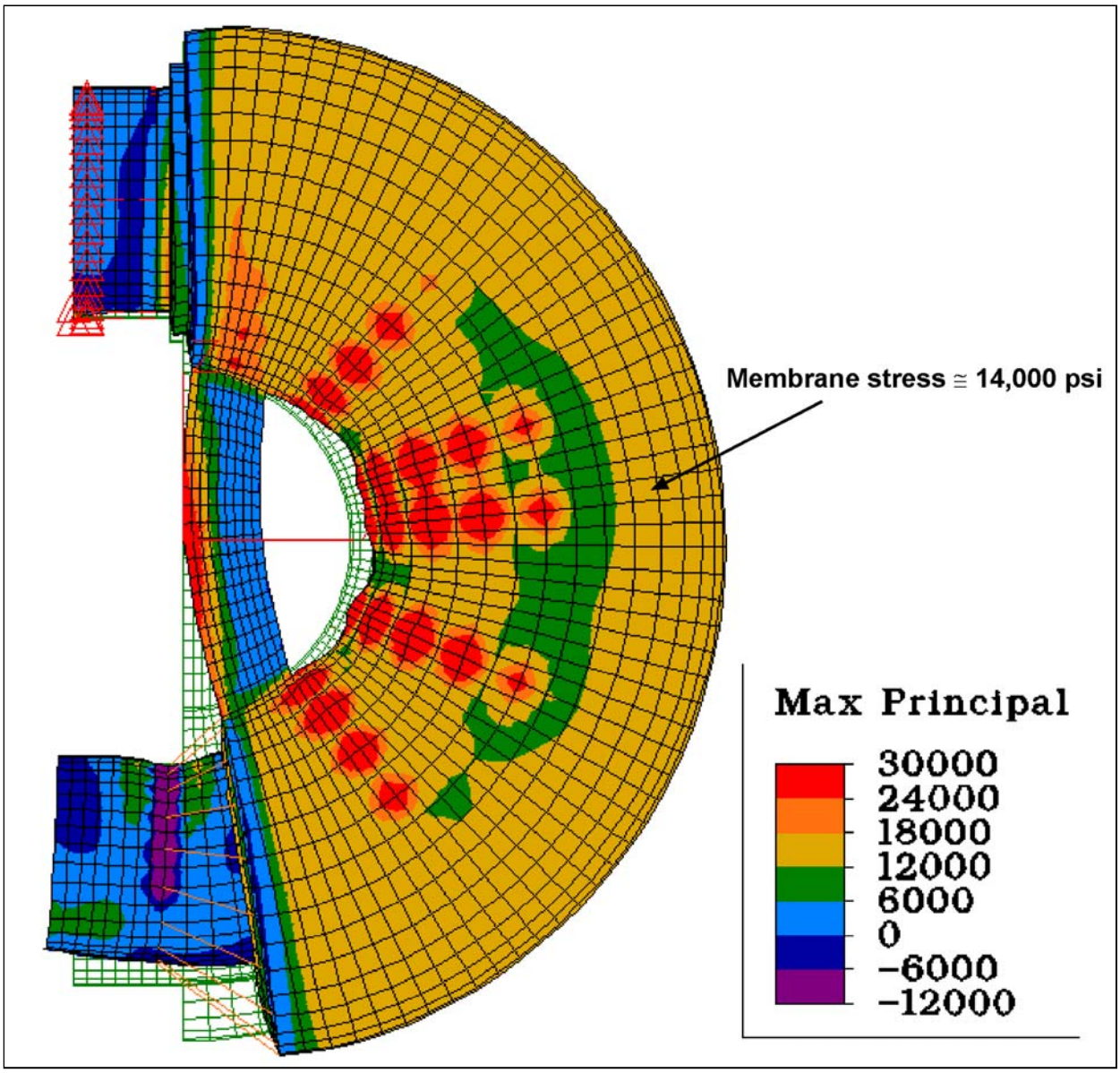

Figure 8 – Stress distribution with 300-psi pressure in Configuration 1.

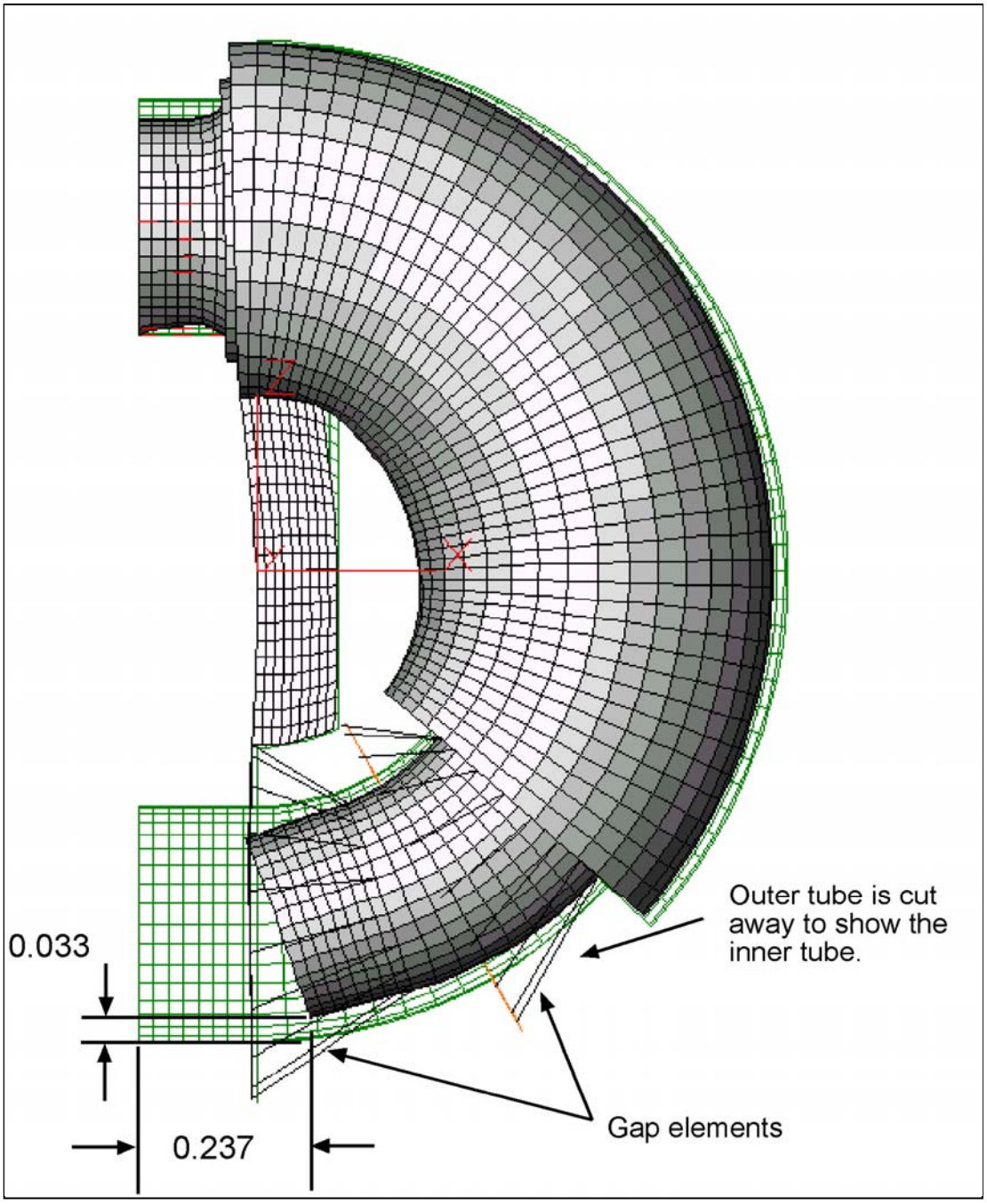

Figure 9 – Deflections in Configuration 1 with inner tube at 4.2 K and remainder at ambient.

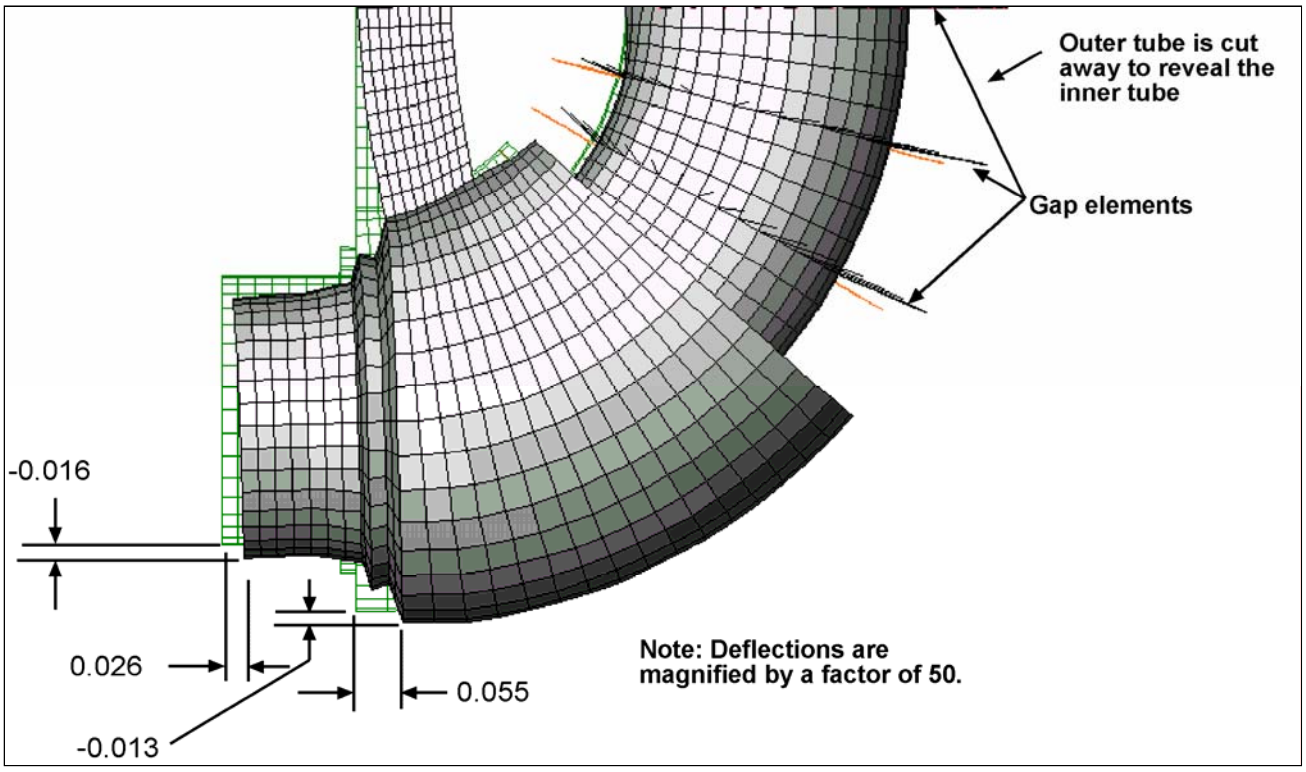

Figure 10 – Configuration 2 deflections with 300-psi pressure.

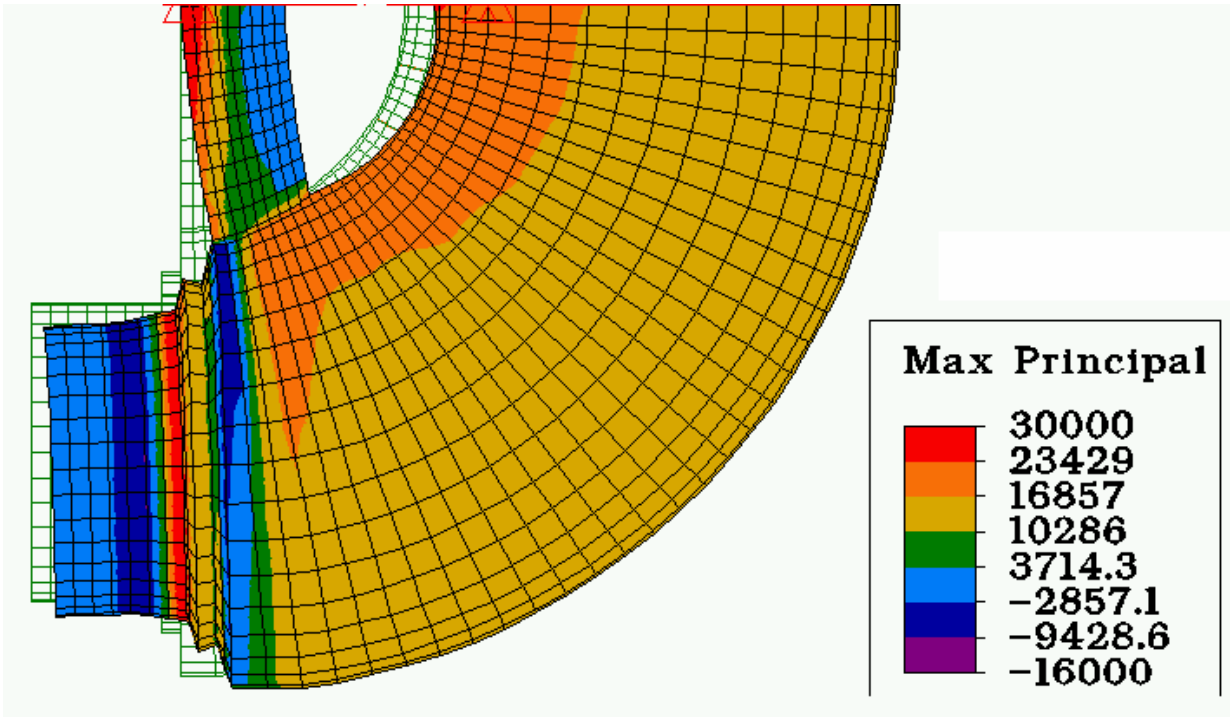

Figure 11 – Stresses in outer tube of Configuration 2 with 300-psi pressure.

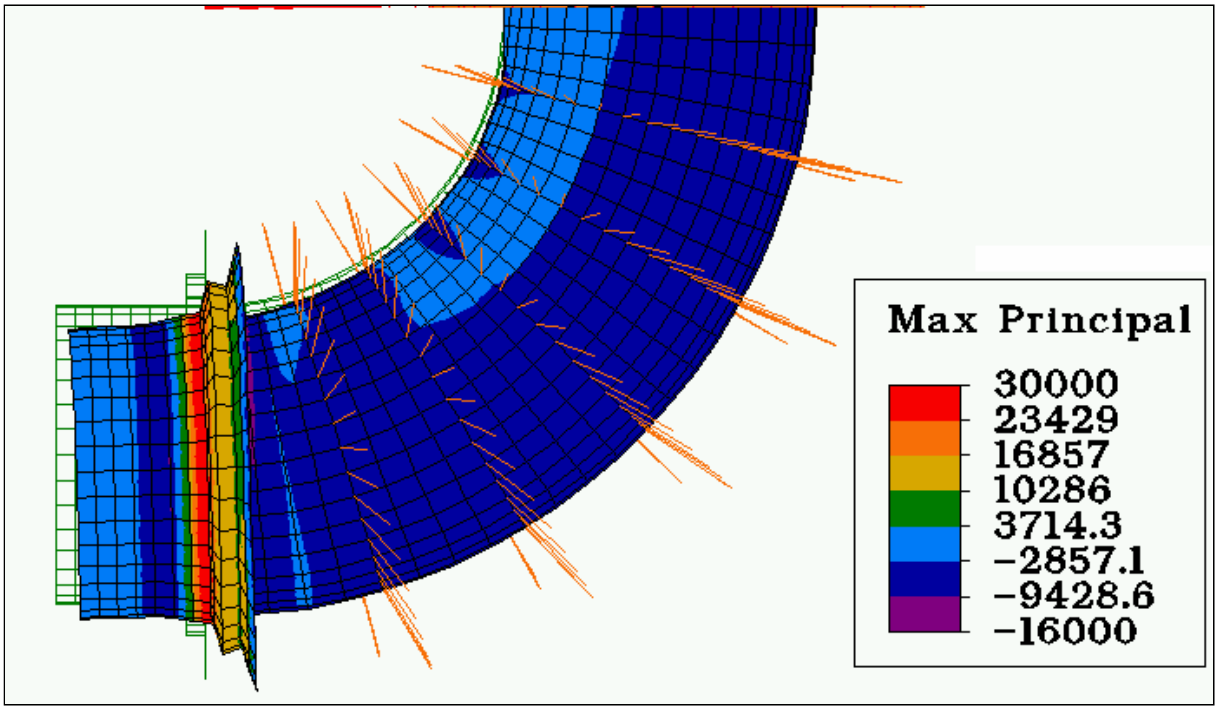

Figure 12 - Stresses in Configuration 2 with 300-psi pressure (Inner tube)

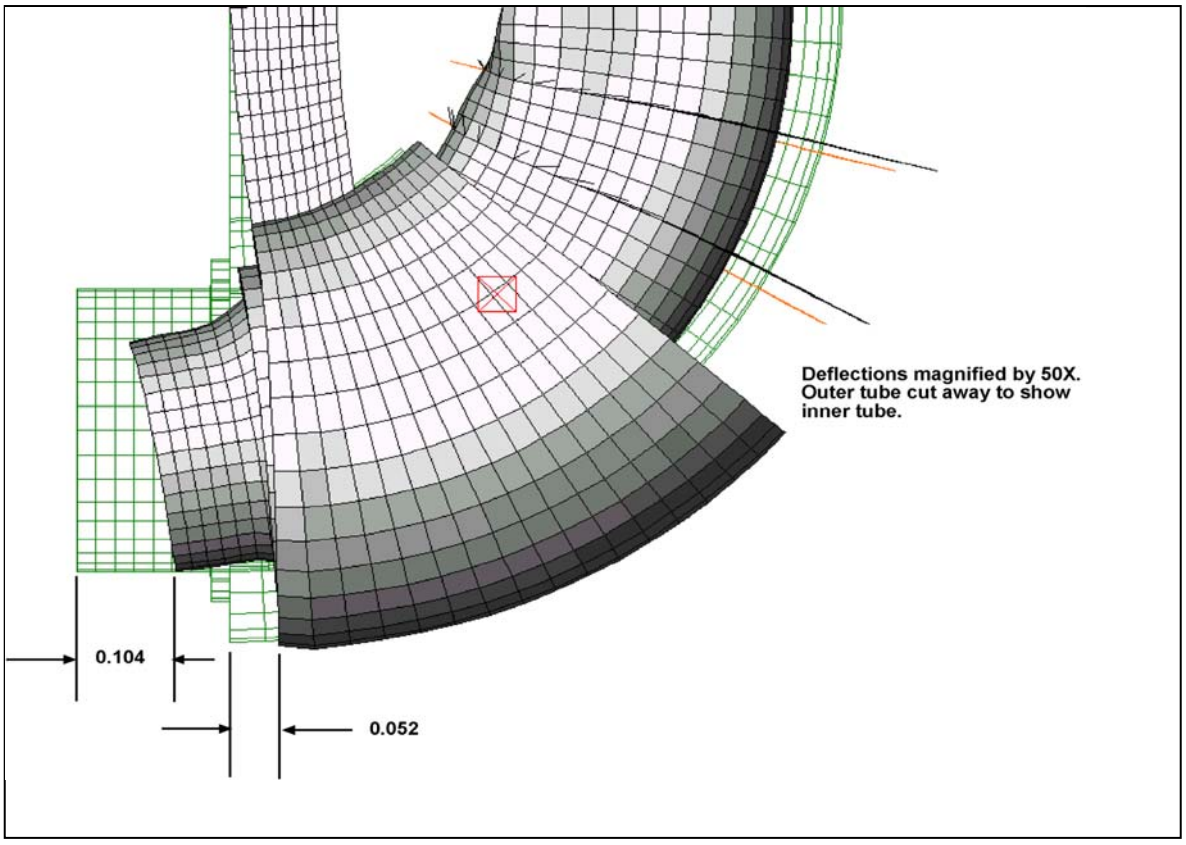

Figure 13 – Deflection with inner tube at 4.2K - in Configuration 2.

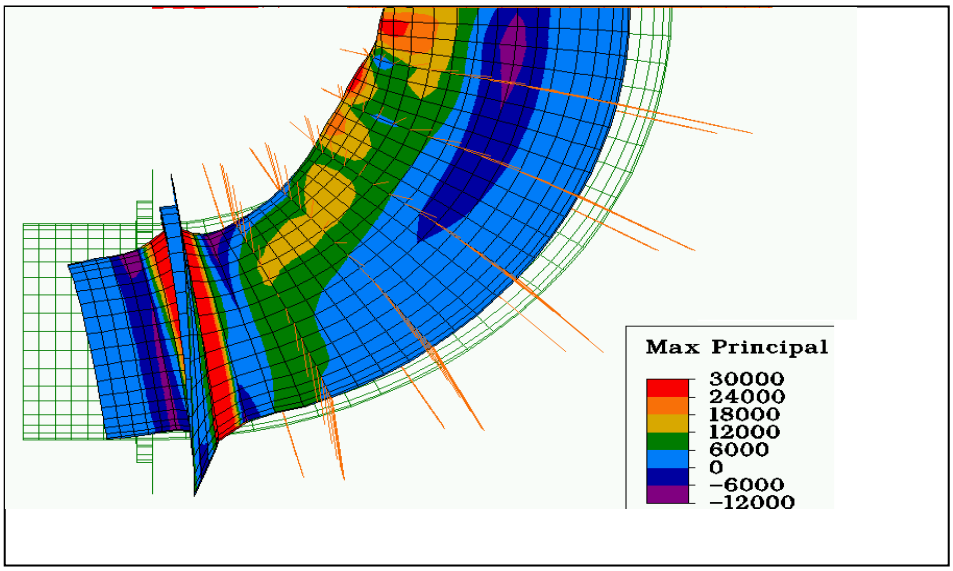

Figure 14 – Stress in Configuration 2 inner tube caused by thermal strain at 4.2K.

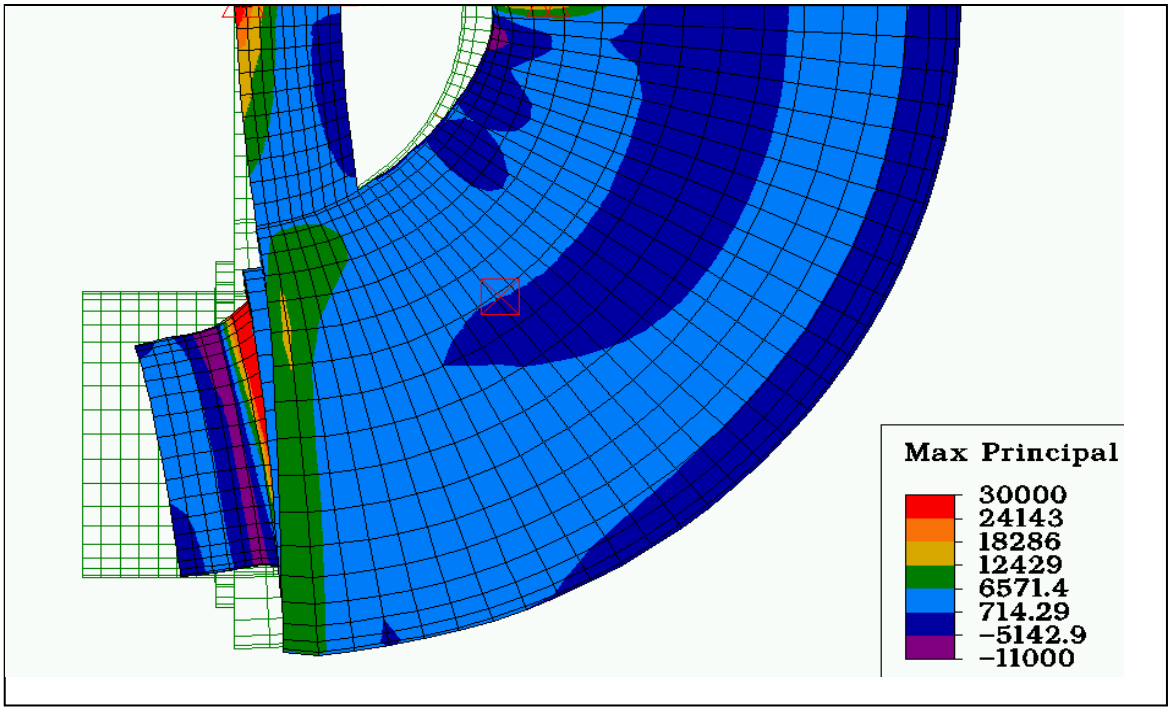

Figure 15 – Stress in Configuration 2 with inner tube at 4.2K

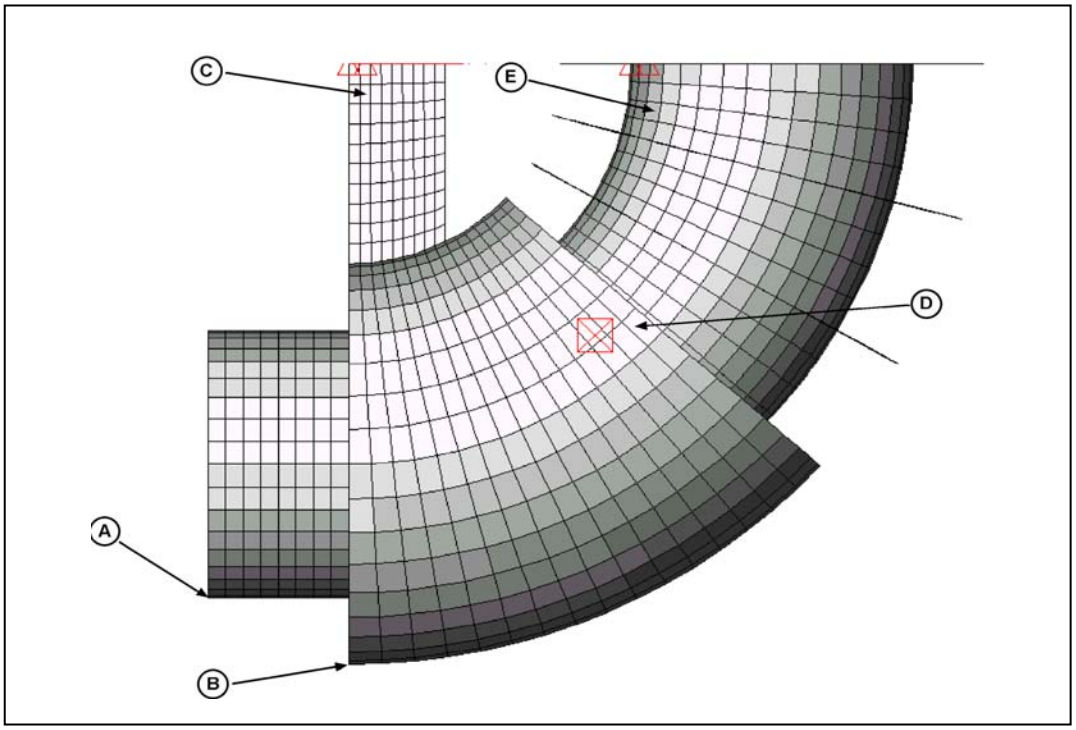

Figure 16 – Locations for deflection and stress output in Table I.